AD-A081 460 REGIS COLL WESTON MA F/G 17/9
DEVELOPMENT AND EVALUATION OF ADAPTIVE TECHNIQUES FOR REDUCING --ETC(U)
SEP 79 D E DONATELLI-DULONG F19628-76-C-0255

UNCLASSIFIED AFGL-TR-79-0256 NL

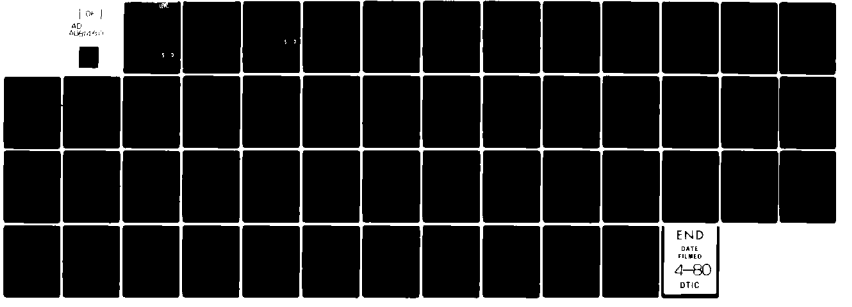

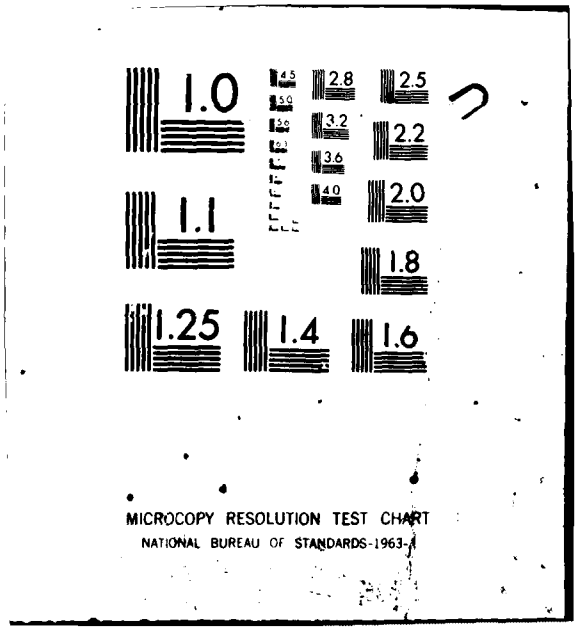
1.0
1.1
1.25
1.4
1.6
1.8
2.0
2.2
2.5
2.8
3.2
3.6
4.0
4.5
5.0
5.6
MICROCOPY RESOLUTION TEST CHART
NATIONAL BUREAU OF STANDARDS-1963-A

AFGL-TR-79-0256

DEVELOPMENT AND EVALUATION OF ADAPTIVE TECHNIQUES FOR REDUCING IONOSPHERIC-INDUCED RADAR TRACKING ERRORS IN REAL TIME

D. E. Donatelli-DuLong

Regis College
235 Wellesley Street
Weston, Massachusetts 02193

30 September 1979

Final Report
1 October 1976 - 30 September 1979

AIR FORCE GEOPHYSICS LABORATORY
AIR FORCE SYSTEMS COMMAND
UNITED STATES AIR FORCE
HANSCOM AFB, MASSACHUSETTS 01731

Unclassified

SECURITY CLASSIFICATION OF THIS PAGE (When Date Entered)

(19) REPORT DOCUMENTATION PAGE	READ INSTRUCTIONS BEFORE COMPLETING FORM
1. REPORT NUMBER (18) AFGL-TR-79-0256	2. GOVT ACCESSION NO. / 3. RECIPIENT'S CATALOG NUMBER (9)
4. TITLE (and Subtitle) (6) Development and Evaluation of Adaptive Techniques for Reducing Ionospheric-Induced Radar Tracking Errors in Real Time,	5. TYPE OF REPORT & PERIOD COVERED Final Report. 1 Oct 76 – 30 SEP 79 / 6. PERFORMING ORG. REPORT NUMBER
7. AUTHOR(s) (10) D. E. Donatelli-DuLong	8. CONTRACT OR GRANT NUMBER(s) (15) F19628-76-C-0255
9. PERFORMING ORGANIZATION NAME AND ADDRESS Regis College 235 Wellesley Street Weston, MA 02193	10. PROGRAM ELEMENT, PROJECT, TASK AREA & WORK UNIT NUMBERS 62101F (16) 4643 01BT (17) 01
11. CONTROLLING OFFICE NAME AND ADDRESS Air Force Geophysics Laboratory Hanscom AFB, Massachusetts 01731 Monitor/Richard Allen/PHP (11)	12. REPORT DATE 30 SEP 79 / 13. NUMBER OF PAGES (12) 51
14. MONITORING AGENCY NAME & ADDRESS (if different from Controlling Office)	15. SECURITY CLASS. (of this report) Unclassified / 15a. DECLASSIFICATION DOWNGRADING SCHEDULE N/A

16. DISTRIBUTION STATEMENT (of this Report)

Approved for public release; distribution unlimited

17. DISTRIBUTION STATEMENT (of the abstract entered in Block 20, if different from Report)

DTIC ELECTE S MAR 6 1980 D B

18. SUPPLEMENTARY NOTES

19. KEY WORDS (Continue on reverse side if necessary and identify by block number)

Ionospheric refraction correction, adapted predictions, space-time correlation cell, TEC r.m.s. variability, radar range error, navigation timing error, adaptive HF, SPADATS range correction

20. ABSTRACT (Continue on reverse side if necessary and identify by block number)

Adaptive procedures, using real time measurements of ionospheric parameters to reduce r.m.s. errors in predictions, are analyzed, addressing both additive and multiplicative processes as contributors to ionospheric variability. A particular procedure is tested using total electron content data from four stations at solar maximum and three stations at solar minimum. Its impact on radar, navigation and communication systems is evaluated, considering diurnal, seasonal and solar cycle effects. A →

DD FORM 1 JAN 73 1473 EDITION OF 1 NOV 65 IS OBSOLETE

Unclassified 801000

SECURITY CLASSIFICATION OF THIS PAGE (When Date Entered)

space-time correlation cell is defined and cell limits established on the basis of temporal and spatial growth rate of r.m.s. residual error. Results indicate that an adapted prediction can significantly improve system performance, particularly in daytime at solar maximum when ionospheric refraction effects are most severe.

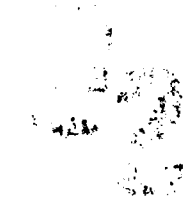

TABLE OF CONTENTS

INTRODUCTION:

Advancements on technology increase the potential for precision in radar navigation and communication systems, but daily variability of the ionosphere continues to be a constraint on achievable system performance. Numerical maps which provide monthly median correction for ionospheric effects have been derived from a world-wide climatology of ionospheric parameters; their use alone reduces the monthly r.m.s. residual error to about 20-25 percent of the median correction in daytime and 30-35 percent at night. Now 20 percent of the monthly median correction for ionospheric effects is often still the dominant error component in systems that are free to calculate performance on a monthly basis; but many present systems cannot tolerate the individual departures of 50 to 200 percent that are averaged away in these monthly statistics. For these precision systems adapted predictions have been proposed which would use various field measurements to make real time corrections for ionospheric effects.

The local ionosphere in the system coverage area is monitored through measurements of ionospheric parameters such as the critical frequency of the F-region (foF2), total electron content (TEC), the gradient in the lower F-region; or through measurements derived from the system itself, such as the signal to noise ratio measured at a distant site and retransmitted to the system control. Some system users may not have the capability of implementing computer models based on world-wide climatology, and instead may use locally monitored TEC or foF2 to estimate monthly median behavior and short term persistence effects. That is, they produce means of several days to predict the subsequent hourly, daily, weekly response of their system to the current state of the ionosphere. If the user is only concerned with ionospheric behavior in the area being monitored by these measurements, such a technique may be sufficient, but if extrapolation in space is necessary, the use of a model is required to account for latitudinal and local time gradients.

Adaptive procedures that use real time observations to reduce average monthly r.m.s. errors in predictions have been examined using foF2 data[1], and TEC data[2,3,4]. These include TEC as derived from measurements of Doppler shift on ensuing passes of the Navy Navigation Satellites (NNSS), and from

---

1. Wilkinson, P.J. (1970): Prediction Limits for foF2. International Solar-Terrestrial Predictions Workshop Proceedings, April 1979, to be published by NOAA, Boulder, Colorado.

2. Donatelli, D.E. and R.S. Allen (1978): Temporal Variability of Ionospheric Refraction Correction. Proc. IES 78, Symposium on the Effect of the Ionosphere on Space and Terrestrial Systems, Editor J.M. Goodman, NRL and ONR, Washington, D.C., 1978: 490-496, #008-051-0069-1.

Faraday rotation measurements using VHF beacons from geostationary satellites. The procedures apply to any type of synoptic data, and rely on a reasonable prediction of the monthly mean of the observations, the standard deviation, and an assumption on the correlation of the observations in the space-time cell being considered. Two basic procedures will be discussed: the first addresses multiplicative processes in the variability of the ionosphere; the second addresses additive processes. In both cases the results of positive and negative correlation are considered.

An evaluation of the procedure is presented considering the case of multiplicative processes. A baseline mapping of monthly mean refraction correction is adapted with real time measurements of TEC; the procedure scales the map of a system coverage area with a ratio of observed to predicted TEC. This ratio is determined at a reference point and extended in space and time. Since any mapping based on climatology must introduce model-dependent bias, an ideal baseline mapping is approached by using the actual mean of the observations in the procedure.

The temporal and spatial growth of the r.m.s. residual error is examined using the concept of a space-time cell, defined as the extension in space and time from a reference point where the residual error is defined as zero, to the limit where the residual error of the adapted map is equivalent to the variance from the baseline prediction. For an individual system, the limit would be modified to lie within the error budget of the system, assuming it is less than the variance.

Since the refraction of a radio signal is directly proportional to the electron content along the ray path, a system user may translate the results to be presented here in terms of system parameters, such as time delay or error in range determination, as follows:

$$\text{Time Delay} = \Delta T = \frac{40.3}{cf^2} \times \text{TEC; in seconds}$$

$$\text{Range Error} = \Delta R = c\Delta T = \frac{40.3}{f^2} \times \text{TEC; in meters}$$

---

3. Leitinger, R., R.S. Allen, D.E. Donatelli, G.K. Hartmann (1978): Adaptive Mapping of Ionospheric Features. Proc. IES 78, Symposium on the Effect of the Ionosphere on Space and Terrestrial Systems, Editor J.M. Goodman, NRL and ONR, Washington, D.C., 1978: 530-537, #008-051-0069-1.

4. Donatelli, D.E. and R.S. Allen (1979): Ionospheric Refractive Correction using an Adaptive Procedure. International Solar-Terrestrial Predictions Workshop Proceedings, April 1979, to be published by NOAA, Boulder, Colorado.

where: f is the frequency of the radio signal
c is the speed of light in a vacuum
TEC is in units of electrons/meter^2 x 10^{16}.

ANALYSIS

The procedure was developed from the assumption that the major components of the daily variability of the ionosphere could be described as large scale, large magnitude fluctuations that are slowly varying, and therefore, reasonably correlated in space and time. These fluctuations result from either multiplicative or additive processes; the analysis is similar in each case. The r.m.s. error when using the adaptive procedure is determined as follows:

$$\chi^2_{R,t} = \frac{\Sigma(O_{R,t} - P_{R,t})^2}{N} \qquad (1)$$

where: $O_{R,t}$ = the observation at the point where the correction is applied

$P_{R,t}$ = the prediction at the point of correction using an observation from a reference point

N = the number of observations

t,R = the time and place of the applied correction, respectively.

This can be expanded to:

$$\chi^2_{R,t} = \sigma^2_{R,t} + \mu^2_{R,t} + \frac{\Sigma}{N}P^2_{R,t} - 2\frac{\Sigma}{N}O_{R,t}P_{R,t} \qquad (2)$$

Assuming a normal distribution with mean μ and variance σ^2, and large N such that $N \simeq N - 1$. $P_R(t)$ is defined by the process being considered, as follows:

Case 1: Multiplicative process

a. positive correlation

$$P_{R,t} = \frac{O_{o,o}}{\mu_{o,o}}\mu_{R,t}$$

b. negative correlation

$$P_{R,t} = 2 - \frac{O_{o,o}}{\mu_{o,o}}\mu_{R,t}$$

Case 2: Additive process

a. positive correlation

$$P_{R,t} = (O_{o,o} - \mu_{o,o}) + \mu_{R,t}$$

b. negative correlation

$$P_{R,t} = (\mu_{o,o} - O_{o,o}) + \mu_{R,t}$$

μ and σ denote the mean and the standard deviation of the observations, respectively. The subscripts o,o and R,t denote the point, in space and time, of reference and of applied correction, respectively.

To evaluate multiplicative processes, first consider case 1a, where by substituting for $P_{R,t}$ and normalizing to the mean, equation (2) becomes:

$$\frac{\chi^2_{R,t}}{\mu^2_{R,t}} = \frac{\sigma^2_{R,t}}{\mu^2_{R,t}} + \frac{\sigma^2_{o,o}}{\mu^2_{o,o}} - 2\left\{\frac{\Sigma O_{o,o} O_{R,t}}{N\mu_{o,o}\mu_{R,t}} - 1\right\} \tag{3}$$

From the definition of the correlation coefficeient, $\rho_R(t)$, it can be shown that:

$$\frac{\Sigma O_{o,o} O_{R,t}}{N\mu_{o,o}\mu_{R,t}} - 1 = \frac{\sigma_{o,o}\sigma_{R,t}}{\mu_{o,o}\mu_{R,t}}\rho_{R,t} \tag{4}$$

Equation (3) can then be written:

$$\frac{\chi^2_{R,t}}{\mu^2_{R,t}} = \frac{\sigma^2_{R,t}}{\mu^2_{R,t}} + \frac{\sigma^2_{o,o}}{\mu^2_{o,o}} - 2\frac{\sigma_{o,o}\sigma_{R,t}}{\mu_{o,o}\mu_{R,t}}\rho_{R,t} \tag{5a}$$

Then by defining:

$$\alpha \equiv \frac{\sigma_{o,o}}{\mu_{o,o}}\frac{\mu_{R,t}}{\sigma_{R,t}} \text{ or } \frac{\sigma_{o,o}}{\mu_{o,o}} \equiv \alpha\frac{\sigma_{R,t}}{\mu_{R,t}}$$

and substituting, equation 5a becomes:

$$\chi^2_{R,t} = \sigma^2_{R,t}\,(1 + \sigma^2 - 2\alpha\rho_{R,t}) \tag{5b}$$

If a negative correlation is known to exist, then $P_{R,t}$ for case 1b is substituted in equation (2) with the following result:

$$\frac{\chi^2_{R,t}}{\mu^2_{R,t}} = \frac{\sigma^2_{R,t}}{\mu^2_{R,t}} + \frac{\sigma^2_{o,o}}{\mu^2_{o,o}} + 2\,\frac{\sigma_{o,o}\sigma_{R,t}}{\mu_{o,o}\mu_{R,t}}\,\rho_{R,t} \tag{6a}$$

Then by introducing α:

$$\chi^2_{R,t} = \sigma^2_{R,t}\,(1 + \alpha^2 + 2\alpha\rho_{R,t}) \tag{6b}$$

When additive processes are being considered, and a positive correlation is assumed, $P_{R,t}$ for case 2a is substituted in equation (2) resulting in the following:

$$\chi^2_{R,t} = \sigma^2_{R,t} + \sigma^2_{o,o} - 2\sigma_{R,t}\sigma_{o,o}\rho_{R,t} \tag{7a}$$

Here define:

$$\beta \equiv \frac{\sigma_{o,o}}{\sigma_{R,t}} \text{ or } \sigma_{o,o} = \beta\sigma_{R,t}$$

Then substitute to arrive at:

$$\chi^2_{R,t} = \sigma^2_{R,t}\,(1 + \beta^2 - 2\beta\rho_{R,t}) \tag{7b}$$

Now when a negative correlation is known to exist, $P_{R,t}$ for case 2b is substituted in equation (2) and the result is:

$$\chi^2_{R,t} = \sigma^2_{R,t} + \sigma^2_{o,o} + 2\sigma_{R,t}\sigma_{o,o}\rho_{R,t} \tag{8a}$$

Then by introducing β:

$$\chi^2_{R,t} = \sigma^2_{R,t}\,(1 + \beta^2 + 2\beta\rho_{R,t}) \tag{8b}$$

The goal of the adaptive procedure is to reduce the system error compared to the average monthly residual error, $\sigma_{R,t}$. The procedure is then considered successful if the following condition is met: $\chi_{R,t} < \sigma_{R,t}$.

For Case 1 (a and b) this condition is met when $\alpha < 2\,|\,\rho_{R,t}|$.

For Case 2 (a and b), the analogous condition is $\beta < 2|\rho_{R,t}|$.

Since α and β can never be negative then $|\rho_{R,t}| > 0$. If $\rho_{R,t} = 0$, then $\chi_{R,t} > \sigma_{R,t}$; if $\alpha = \beta = 0$, then $\chi_{R,t} = \sigma_{R,t}$. In these cases the procedure should not be used.

In summary, for the multiplicative process, the procedure is effective if $|1| \geq |\rho_{R,t}| > \alpha/2 > 0$

and for the additive process, if

$|1| \geq |\rho_{R,t}| > \beta/2 > 0.$

Now consider the ideal cases of perfect correlation, $\rho_{R,t} = 1$ (case a) and anti-correlation, $\rho_{R,t} = -1$ (case b):

For cases 1a and 1b, equations 5a and 6a reduce to:

$$\frac{\chi_{R,t}}{\mu_{R,t}} = \left| \frac{\sigma_{R,t}}{\mu_{R,t}} - \frac{\sigma_{o,o}}{\mu_{o,o}} \right| \tag{9a}$$

and 5b and 6b reduce to:

$$\chi_{R,t} = \sigma_{R,t} |1 - \alpha| \tag{9b}$$

then the procedure is successful within the limits:

$$0 < \frac{\sigma_{o,o}}{\mu_{o,o}} < 2 \frac{\sigma_{R,t}}{\mu_{R,t}}$$

$$0 < \alpha < 2.$$

For cases 2a and 2b, equations 7a and 8a reduce to:

$$\chi_{R,t} = |\sigma_{R,t} - \sigma_{o,o}| \tag{10a}$$

and 7b and 8b reduce to:

$$\chi_{R,t} = \sigma_{R,t} |1 - \beta| \tag{10b}$$

setting the limits as:

$$0 < \sigma_{o,o} < 2\sigma_{R,t}$$

or $0 < \beta < 2.$

EVALUATION

From this analysis it can be seen that, if perfect correlation or anti-correlation exists, the success of the adaptive procedure depends on the absolute difference in the percentage standard deviation with respect to the mean between the reference point and the point of applied correction ("point" referring to a location in both time and space), for a multiplicative process, equation 9a.

For an additive process it is simply the difference in the standard deviation between points, equation 10a. Then, it is possible, by comparing the absolute and percentage standard deviations between relevant points, to estimate the potential success of an adaptive procedure, and even to determine whether multiplicative or additive processes dominate. For this type of evaluation to be meaningful, there should be simultaneous data available from several locations within a typical system coverage area, encompassing diurnal, seasonal and solar cycle variations.

The TEC data for this study were obtained from measurements of the Faraday rotation of signals from beacons of geostationary satellites[5]. The available data were in two sets: the first, from four stations for 1968-69; the second, from three stations for 1974-76. The location of monitoring sites, the geostationary satellite that was monitored, and the location of the 420 km. sub-ionospheric point along the ray path, are presented in Table I.

TABLE I. LOCATION OF TEC MEASUREMENTS

Station	Satellite	Sub-ionospheric Point
1968 - 69		
Hamilton, Massachusetts (HAM)	ATS-3	39N. 289E.
Urbana, Illinois (URB)	ATS-3	36N. 274E.
Stanford, California (STA)	ATS-1	34N. 234E.
Edmonton, Alberta (EDM)	ATS-1	47N. 239E.
1974 - 76		
Goose Bay, Labrador (GSB)	ATS-3	48N. 289E.
Hamilton, Massachusetts (HAM)	ATS-3	39N. 289E.
Kennedy Space Flight Center, Florida (KSF)	ATS-3	26N. 280E.

5. Titheridge, J.E. (1972): Determination of Ionospheric Electron Content from the Faraday Rotation of Geostationary Satellite Signals. Planetary and Space Science, 20: 353-369.

The first set of data represent the recent solar maximum, and the second, the subsequent solar minimum. These data provide a good basis for evaluation of the average behavior of this type of procedure since this solar cycle closely approximates the average of the past 20 solar cycles with $\bar{R}_z$ = 110, $\bar{S}$ = 155 at maximum, and $\bar{R}_z$ = 10, $\bar{S}$ = 71 at minimum, where $\bar{R}_z$ and $\bar{S}$ are the twelve-month running mean sunspot number and solar flux at 2800 Mhz, respectively. To estimate TEC for other values of $\bar{R}_z$ (or $\bar{S}$) it is still possible to interpolate or extrapolate to a reasonable approximation by assuming a linear relationship between $\bar{R}_z$ (or $\bar{S}$) and TEC.[6]

To estimate the potential of adaptive procedures, first consider multiplicative processes, as defined by cases 1a and 1b with $\rho = 1$ or $\rho = -1$, respectively. In this case the percentage r.m.s. error, $\chi_{R,t}/\mu_{R,t}$, is estimated by equation 9a, which requires knowledge of the percentage standard deviation for the reference point and the point of applied correction. This percentage was calculated for each month of data at each location in Table I. The results are shown in Figures 1a,b,c,d for the months of January, April, July and October, respectively, for the years 1969 and 1975, allowing examination of diurnal, seasonal, and solar cycle effects. For an operational-type assessment it seemed more appropriate to plot the curves in Universal Time. From these curves it can be determined between which locations and during which times of day, season and solar cycle, the minimum conditions are met for using the adaptive procedure.

The growth of the percentage error in time, at any location, may be estimated by taking progressive differences along the curve for a particular location from some choice of reference time on that curve. When

$$\left|\frac{\sigma_{0,t}}{\mu_{0,t}} - \frac{\sigma_{0,0}}{\mu_{0,0}}\right| = \frac{\sigma_{0,t}}{\mu_{0,t}}$$

the limit of a time cell is defined. In the same manner, the limit for a spacetime cell is defined by taking progressive differences in time and location from some defined reference point, to the point where

$$\left|\frac{\sigma_{R,t}}{\mu_{R,t}} - \frac{\sigma_{0,0}}{\mu_{0,0}}\right| = \frac{\sigma_{R,t}}{\mu_{R,t}} \quad .$$

One of the limitations on space-time cell extent that may be determinted from these curves, is that large errors can be generated when a scaling factor from nighttime is used across the sunrise terminator to adapt daytime predictions. This is a greater concern at solar minimum than at solar maximum since the percentage variability fluctuates more radically; with the lower mean values at solar minimum a small absolute variation of TEC will produce a large percentage variation, particularly at nighttime.

---

6. DuLong, D.D. (1977): Reduction of the Uncertainty of Radar Range Correction. AFGL-TR-77-0125, DDC# ADA 046166.

In general, the extended space-time cells that are possible at solar maximum must be reduced at solar minimum. However, the remaining variability, in TEC units (electrons/meter^2 x 10^{16}), is still less at solar minimum. Note that it is χ_t, not the percentage $\chi_{R,t}/\mu_{R,t}$ that is of primary concern to systems.

When additive processes are considered, the potential of the adaptive technique may be estimated using figures 2a,b,c,d. These are the curves for the standard deviation in TEC units for the months and locations of figure 1. Again, the process is considered for $\rho = 1$ or $\rho = -1$, where the error, $\chi_{R,t}$, is defined by equation 10a. From these curves $\chi_{R,t}$ is obtained directly in TEC units by taking differences between points, analogous to figure 1. This figure indicates that variability in terms of additive processes may provide a better description of nighttime and solar minimum conditions, but would be less descriptive of daytime, particularly at solar maximum.

ADAPTIVE PROCEDURE

Since the daytime error at solar maximum causes the severest system problems, it was decided that this study should examine the adaptive procedure for a multiplicative process in detail, specifically case 1a. The assumption here is that within the available data base, the correlation is expected to monotonically decrease to zero with distance, and negative correlation is not anticipated. Based on correlation studies[7,8] this is a reasonable assumption, particularly at mid-latitudes.

The procedure is initiated by obtaining a measurement of TEC at a reference point ($O_{0,0}$) determining a scaling factor from the ratio of the observation to the baseline prediction for the reference point ($M_{0,0}$) and scaling the baseline map over the coverage area for a succeeding time period. The adapted prediction ($P_{R,t}$) at a remote time and/or site is then:

$P_{R,t} = \frac{O_{0,0}}{M_{0,0}} M_{R,t}$ where $M_{R,t}$ is the baseline prediction at the remote time and/or site. As noted previously, the actual monthly mean is used for the baseline prediction at each site to remove any model-dependent error from the ensuing results. Thus, from case 1a:

$P_{R,t} = \frac{O_{0,0}}{\mu_{0,0}} \mu_{R,t}$. The TEC data are reduced at 15-minute intervals. The

---

7. Rush, C.M. (1976): An Ionospheric Observation Network for use in Short-Term Propagation Predictions. Telecommunication Journal, 43 (VIII): 544-549.

8. Klobuchar, J.A. and J.M. Johanson (1977): Correlation Distance of Mean Daytime Electron Content. AFGL-TR-77-0185, DDC# ADA 048117.

adapted prediction is applied at these intervals over several hours, at all locations having simultaneous data. Comparisons are made with the corresponding observations, and the r.m.s. error, $\chi_{R,t}$ is computed each month at each location, at each 15-minute increment from the same reference times each day.

TIME CELL RESULTS

The potential of this simple adaptive technique for reducing the r.m.s. error of a refractive correction is demonstrated in Figure 3, using data from Hamilton, Massachusetts for January, 1969. For this case the local ionospheric measurements are used to predict their subsequent temporal behavior, so there is no spatial component in the results. In figure 3a the observed 10-day mean is used to map into future times; in figure 3b a standard AFGL model based on the ionospheric climatology contained in world maps[9] is the baseline. Note that the diurnal shape derived from the AFGL model differs from the observed ionospheric behavior. The outer scale on the figures, to be used for the means, is four times greater than the inner scale, which is to be used for the standard deviations with respect to the means and for the r.m.s. error of the adapted predictions with respect to the observations. Although there is up to 20 percent difference between the AFGL predicted and the observed mean, the monthly standard deviation with respect to each mean is comparable. Thus on the basis of using a monthly prediction without adaption, the world-wide monthly median climatology predicts as well as the mean itself.

The growth of the r.m.s. error of the adapted prediction, $\chi_{H,t}$ is described by the thin lines originating at a convenient 2 hour interval, where $\chi_{H,t_o} = 0$. In 3a, $\chi_{H,t}$ extends in time from $t = t_o$ to $t = t_o + 3$ hours; in 3b from $t = 0$ to $t = t_o$ and held constant over the 3 or 12 hour time cell; only the scaling of the mean ($\mu_{H,t}$) or the predicted mean ($M_{H,t}$) is progressed with time.

The dashed lines define the residual error for a 3 hour time cell (χ_H, $t_o + 3h$) and indicate that a scaling factor that is 3 hours old is useful throughout the daytime hours, unless it was determined prior to sunrise and used thereafter. The difference between 1a and 1b is the model-dependent error, most evident in the sunrise area. Comparing these curves with the standard deviation ($\sigma_{H,t}$) with respect to the monthly mean and the standard deviation ($S_{H,t}$) with respect to the model prediction, it is apparent

9. Barghausen, A.F., J.W. Finney, L.L. Proctor, L.D. Schultz (1969): Prediction Long-Term Operational Parameters of High-Frequency Sky-Wave Telecommunications Systems. ESSA Technical Report ERL 110-ITS-78.

that the time cell in which an adapted prediction, based on a single scaling factor, is useful, is bound by the reference time on one end and the succeeding solar terminator on the other. (An analysis of $\chi_{R,t}$ for case 1a, that includes the effect of the model bias can be found in Appendix A.

The analysis in this report has assumed the data follows a normal distribution. In reality, however, it is somewhat skewed toward higher values in daytime. Therefore, a model which tends to predict a mean that is slightly greater than the observed mean in daytime will often succeed in reducing the monthly variance at that time.

In a previous study[6] the performance of this adaptive technique, predicting only in time for a fixed location, was examined using all of the archive data of TEC from Hamilton, Massachusetts, 1969 through 1976. Table 2 summarizes these results for the daytime and nighttime maxima, averaged over season, at both solar maximum and minimum, in TEC units of electrons/meter^2 x 10^{16}. This table shows that an adapted prediction can reduce the residual error by 60 percent in a one hour time cell and still by as much as 30 percent in a three hour time cell for daytime solar maximum.

The time cell for useful adapted predictions is determined by the correlation times of fluctuations in TEC. Since the basic data for this study were reduced at 15 minute intervals, fluctuations with periods less than 30 minutes are not observable. Their amplitude is assumed to be much smaller than the longer period variations that are being tracked here. The present simple adaptive technique, predicting persistence of a direction of variation for times of 15 minutes to three hours, tends to mitigate against just those long period TEC variations which seem to be a major component at solar maximum. Thus this adaptive procedure is most successful at solar maximum, yet the residual is of the same absolute magnitude as the residual at solar minimum. This suggests that the short period variations of TEC predominate at solar minimum, and are still present with the same amplitude at solar maximum, masked by the characteristic larger scale variations.

During sunrise and sunset periods, the effects of production and loss create gradients that dominate all other fluctuations. Similar gradients may occur during magnetic disturbance, particularly in the region of the auroral zone and the trough in high and mid-latitutdes. The rate at which these changes occur would determine the time cells for these periods. This is illustrated in figure 2 where the observed TEC is compared to the results of using adapted predictions on a highly disturbed day at Hamilton, Massachusetts.

Figure 4a compares the prediction for the month, $\mu_{H,t}$ the observed TEC for the day, $O_{H,t}$ the adapted prediction for a 30 minute time cell, P_{H,t_o} + 30m and a 3-hour time cell, P_{H,t_o} + 3h. Figure 4b shows the differ-

---

6. DuLong, D.D. (1977): Reduction of the Uncertainty of Radar Range Correction. AFGL-TR-77-0125, DDC# ADA 046166.

TABLE 2. RESIDUAL ERRORS IN TEC PREDICTION TIME CELLS

	WINTER		VERNAL EQUINOX		SUMMER		AUTUMNAL EQUINOX	
	DAY	NIGHT	DAY	NIGHT	DAY	NIGHT	DAY	NIGHT
	Solar Maximum ($\bar{R}_z$ = 110; $\bar{S}$ = 155)							
$\mu_{H,t}$	34.4	5.7	44.8	8.2	25.4	8.2	41.1	6.7
$\sigma_{H,t}$	6.0	1.8	7.8	2.5	4.0	2.2	7.8	2.2
χ_{H,t_o+3h}	4.0	1.5	4.5	1.5	2.7	1.5	4.0	1.8
χ_{H,t_o+1h}	2.2	1.0	2.5	1.0	1.6	1.2	1.6	0.7
χ_{H,t_o+30m}	1.5	0.6	1.5	0.6	1.2	0.6	1.3	0.6
	Solar Minimum ($\bar{R}_z$ = 10; $\bar{S}$ = 71)							
$\mu_{H,t}$	10.5	1.5	10.5	1.5	9.0	2.1	11.2	2.1
$\sigma_{H,t}$	1.8	0.6	2.5	0.6	1.5	0.5	1.5	0.6
χ_{H,t_o+3h}	1.8	0.9	2.1	0.5	1.5	0.5	2.1	0.6
χ_{H,t_o+1h}	1.2	0.3	1.2	0.1	0.6	0.3	1.2	0.3
χ_{H,t_o+30m}	0.9	0.1	0.6	0.1	0.4	0.1	0.6	0.1

The symbols used represent the following:

$\mu_{H,t}$ - The mean value of TEC

$\sigma_{H,t}$ - The r.m.s. deviation of TEC from the mean, representing the day-to-day variability of the ionosphere

χ_{H,t_o+3h} - The residual error using an adapted prediction in a 3-hour time cell

χ_{H,t_o+1h} - The residual error using an adapted prediction in a 1-hour time cell

χ_{H,t_o+30m} - The residual error using an adapted prediction in a 30-minute time cell.

ences between the observed TEC and the predictions in each case. The error using the 3-hour time cell $\left|O_{H,t_o+3h}-P_{H,t_o+3h}\right|$ is equivalent in magnitude to that using the monthly mean $\left|O_{H,t}-\mu_{H,t}\right|$, but large excursions have been introduced at time periods when they would otherwise not exist. The adapted prediction using a 30 minute time cell, χ_{H,t_o+30m}, provides a 60 percent reduction in the maximum error despite the steep gradients in TEC on this disturbed day.

SPACE-TIME CELL RESULTS

The preceding results assess the adapted prediction when applied at the reference location, progressed in time, thus including only a temporal component of variability. A more valid assessment of this procedure requires inclusion of the spatial component as well. Spatial variations have been previously examined[8,10,11] using data from the TRANSIT satellites reduced to provide TEC along the satellite path, and TEC measurements from several closely spaced monitors of the ATS-6 geostationary satellite. The variation of ionospheric features and some of the implications of attempting to track these features in space and time were considered and will be further examined here.

The following figures represent the actual impact on systems of the use of this procedure. It will be seen that, qualitatively the results agree with the estimates inferred in figure 1. Figures 5-8 present the 1969 data for the months of January, April, July and October, respectively, and the results of its use in the adaptive procedure; figures 9-12 present the 1975 data for the same months in the same manner. The (a) figures, 5-12, compare the mean, $\mu_{R,t}$, standard deviation, $\sigma_{R,t}$, and the residual error minute, (χ_{R,t_o+15m}), 1-hour (χ_{R,t_o+1h}), and 3-hour (χ_{R,t_o+3h}) time cell at each of the stations in each set of data. The (b) figures, 5-12, compare the standard deviation ($\sigma_{R,t}$) for each station with the residual error for a 15-minute (χ_{R,t_o+15m}) 1-hour (χ_{R,t_o+1h}) and 3-hour (χ_{R,t_o+3h}) space-time cell, the spatial reference being one or two of the other stations within the set for the year.

---

8. Klobuchar, J.A. and J.M. Johanson (1977): Correlation Distance of Mean Daytime Electron Content. AFGL-TR-77-0185, DDC# ADA 048117.

10. Allen, R.S. (1977): Considerations Relative to Adapting TRANSIT Observations to Predicting Radar Range Corrections. AFGL-TR-77-0004, DDC# ADA 038238.

11. Davies, K., Degenhardt, G.K. Hartmann, R. Leitinger, (1977): Electron Content Measurements over the U.S., Joint Radio Beacon Program NOAA/MPAE/GRAZ, Station Report ATS-6°, 94°W., Edited by Max Planck Institut für Aeronomie, Lindau, West Germany.

Since the local time variation at each location is inherent in the mean, the variations being tracked by this procedure need not be local time dependent. It can be seen that the results using a 15-minute time cell when projecting in space, are similar or slightly better than using a 1-hour, and consistently better than using a 3-hour time cell. This is independent of the distances and directions considered here. It should be noted, (see figure 3) that the error growth rate is greatest during the first hour and tends to decrease thereafter. The actual error maximizes and minimizes where the changes in variance are zero, near the midday peak and nighttime minimum, respectively.

Direct quantitative comparisons are not possible between the 1969 and 1975 data since the spatial coherence in latitude is less than in longitude. The station-pairs GSB-HAM and HAM-KSF of the 1975 data have latitudinal separations that are equal to, or greater than, their longitudinal separations. This is also true for the 1969 STA-EDM station-pair, but for the HAM-URB and URB-STA station-pairs, the longitudinal exceeds the latitudinal separations. Therefore, only the 1969 STA-EDM station-pair results may be qualitatively compared to the 1975 results for an evaluation of solar cycle variation. However, the 1969 and 1975 Hamilton results may be quantitatively compared.

At solar maximum an improvement of 50 percent or more is achievable in daytime within most of the space-time cells presented here; at solar minimum this is only achievable in daytime within a space-time cell with a 1-hour temporal limit. Some degree of improvement is also possible at nighttime, solar maximum; but at solar minimum nighttime, new errors may be introduced with this procedure. This was anticipated since it is assumed that additive, rather than multiplicative, processes dominate at nighttime and at solar minimum.

ESTABLISHING LIMITS FOR A SPACE-TIME CELL

An approximation for space-time cells is suggested by the results of correlation studies[7,8]. For northern mid-latitude regions, these indicate a ratio of 1:2 between latitude and longitude correlation distances in degrees. Therefore, an ellipse with an axial ration of 1:2 could be used to describe the spatial extent of an applied correction. While the axial ratio would remain constant, the spatial extent, in kilometers, would decay in time. The initial distance would be set by the desired accuracy, and assuming space-time equivalence in longitude.

---

7. Rush, C.M. (1976). An Ionospheric Observation Network for use in Short-Term Propagatior Predictions. Telecommunication Journal, 43 (VIII): 544-549.

8. Klobuchar, J.A. and J.M. Johanson (1977): Correlation Distance of Mean Daytime Electron Content. AFGL-TR-77-0185, DDC# ADA 048117.

This concept may be valid for tracking features even when their growth and damping rates, in space and time, are not explicitly defined. The features observed in Figure 4, which are apt to be confined to a particular local time and magnetic field shell sector, are an example. Note the error of the 30-minute time cell prediction in Figure 4. If this error is within the tolerance of a hypothetical system, the instantaneous boundary of a space-time cell can be defined by a 30-minute equivalent longitude, 7.5 degrees. At Hamilton latitudes this would represent a 645 km East-West axis and a 420 km North-South axis. If a correction is applied at a later time, this ellipse is reduced; for example, 15-minutes after the initial observation the East-West axis would be reduced to 323 km and the North-South to 210 km. At the end of 30-minutes the correction would only apply at the location of the initial observation.

The general case is seen in figures 5-8 where a reduction in variance of 50 percent at solar maximum in daytime can be achieved within a 3-hour time cell, or equivalently, 45^{o} longitude. This is equivalent to the URB-STA station-pair. An observation at Urbana can be used instantaneously to provide an adapted prediction for Stanford, but this spatial extent would decay such that after 3 hours, the adapted prediction would apply only to Urbana itself.

The extent of the space-time cells is greatest at solar maximum daytime when large-scale, long period variations predominate and systems are most concerned in an r.m.s. sense. For systems that are vulnerable to individual features, such as those of figure 4, the extent of the space-time cell must be modified accordingly.

CONCLUSION

When using adapted predictions analysis of r.m.s. error must be based on whether the dominant features are created by additive or multiplicative processes, and whether their extended effects are positively or negatively correlated. From this analysis it was determined that the r.m.s. error for additive processes is dependent on the absolute difference in the standard deviation of the two space-time points under consideration. For a multiplicative process the absolute difference in percentage standard deviation with respect to the mean is the related parameter. A comparison of these parameters for the available data indicated that for the solar maximum period, when ionospheric refraction effects on systems are the most severe, multiplicative processes dominate.

Evaluation of the adaptive procedure required that data be confined to a region typical of a system coverage area. The available data were limited to the northern mid-latitude American sector. From correlation studies it was deemed reasonable to assume a positive correlation throughout the region. Thus it was decided to evaluate, in detail, an adaptive procedure that considered multiplicative processes with positive correlation. The required condition was shown to be $1 \geq \rho_{R,t} > \frac{\alpha}{2} > 0$

where: $\rho_{R,t}$ is the correlation coefficient between points and

α is the ratio of the percentage r.m.s. deviation at the reference point to that at the point of applied correction.

In daytime an improvement of 50 percent is readily achievable: at solar maximum within a 3-hour time cell; at solar simimum within a 1-hour time cell. At nighttime, the percentage r.m.s. deviation is usually greater than daytime, but the absolute deviation is less; therefore, the need for correction is not as crucial. However, if adapted predictions are used, a scaling factor obtained at nighttime should not be projected across the sunrise terminator, as the rapid change in percentage r.m.s. deviation during the sunrise growth period introduces errors. The sunset decay period is less critical since the percentage deviation usually increases at nighttime, therefore α would decrease, allowing a greater range for $\rho_{R,t}$, thereby increasing the probability that the requirement $\rho_{R,t} > \frac{\alpha}{2}$ will be met.

A space-time cell has been defined in terms of an ellipse of constant axial ratio, with a spatial extent that decays with time. It was found that space-time cells with an extent of several thousand kilometers, or several hours, or an equivalent space-time combination, are operationally useful at solar maximum. At solar minimum the absolute value of the r.m.s. deviation is low, therefore the need for correction is less critical. For example, the residual error, using a one-hour time cell at solar maximum, is equivalent to the average monthly variance at solar minimum. Therefore, the adaptiveprocedure succeeds in reducing the error at solar maximum to the lower impact solar minimum levels.

Acknowledgements

The author would like to thank Mr. J. Klobuchar of AFGL for the use of the TEC data and Mr. R. Allen for his many helpful discussions.

This work was supported by Air Force Contract F19628-76-C-0255.

Appendix A

For actual system use, the monthly mean ionospheric behavior would be predicted by a numerical model derived from world-wide climatology. Any model has some inherent bias which may have little consequence on r.m.s. error when the primary concern is predicting the mean behavior, but, as shown in Figure 3b, this bias can effect the adaptive procedure. The following derivation will provide some perspective on the import of this bias.

The r.m.s. error is defined as:

$$\chi^2_{R,t} = \frac{\Sigma}{N} (O_{R;t} - P_{R,t})^2 \tag{A1}$$

where $P_{R,t}$ is the prediction of the adaptive procedure. For the case of a multiplicative process within an area of positive correlation, which is the only case we will examine here:

$$P_{R,t} = \frac{O_{o,o}}{M_{o,o}} M_{R,t} \tag{A2}$$

where: M is the mean as predicted by the model and the subscripts o,o and R,t denote the reference point and the point of applied correction, respectively, in space and time.

Substituting this in equation A1 and expanding:

$$\chi^2_{R,t} = \frac{\Sigma O^2_{R,t}}{N} + \frac{M^2_{R,t}}{M^2_{o,o}} \frac{\Sigma O^2_{o,o}}{N} - 2 \frac{M_{R,t}}{M_{o,o}} \frac{\Sigma O_{R,t} O_{o,o}}{N} \tag{A3}$$

then substitute $\sigma_{R,t}, \sigma_{o,o}$, and $\rho_{R,t}$ in equation (A3) to arrive at:

$$\chi^2_{R,t} = \sigma^2_{R,t} + \mu^2_{R,t} + \frac{M^2_{R,t}}{M^2_{o,o}} (\sigma^2_{o,o} + \mu^2_{o,o}) - 2 \frac{M_{R,t}}{M_{o,o}} (\sigma_{R,t}\sigma_{o,o}\rho_{R,t} + \mu_{o,o}\mu_{R,t}) \tag{A4}$$

To parallel case 1a in the text, normalize to the observed mean:

$$\frac{\chi^2_{R,t}}{\mu^2_{R,t}} = \frac{\sigma^2_{R,t}}{\mu^2_{R,t}} + 1 + \frac{M^2_{R,t}}{\mu^2_{R,t}} \frac{\mu^2_{o,o}}{M^2_{o,o}} \left(\frac{\sigma^2_{o,o}}{\mu^2_{o,o}} + 1 \right) - 2 \frac{M_{R,t}}{\mu^2_{R,t}} \frac{\mu_{o,o}}{M_{o,o}} \left(\frac{\sigma_{R,t}}{\mu_{R,t}} \frac{\sigma_{o,o}}{\mu_{o,o}} \rho_{R,t} + 1 \right) \tag{A5}$$

Now define the model bias, B, such that

$$B_{o,o} = \frac{M_{o,o}}{\mu_{o,o}}; \quad B_{R,t} = \frac{M_{R,t}}{\mu_{R,t}}$$

Take $\rho_{R,t} = 1$, and substituting $B_{o,o}$ and $B_{R,t}$:

$$\frac{\chi^2_{R,t}}{\mu^2_{R,t}} = \left\{\frac{\sigma_{R,t}}{\mu_{R,t}} - \frac{B_{R,t}}{B_{o,o}}\frac{\sigma_{o,o}}{\mu_{o,o}}\right\}^2 + \left\{1 - \frac{B_{R,t}}{B_{o,o}}\right\}^2 \qquad \text{(A6)}$$

It can be seen immediately that if $B_{R,t} = B_{o,o}$, that is, if the model bias does not vary between the points being considered, use of the model will be as effective as the use of the observed mean in the adaptive procedure. However, empirical models are biased by their data base implying preferred regions and times where a higher degree of accuracy is attainable.

Figure Captions

Figure 1a - The diurnal curves of percentage standard deviation in TEC for the month of January at four stations in 1969 and three stations in 1975.

Figure 1b - Same as 1a but for the month of April.

Figure 1c - Same as 1a but for the month of July.

Figure 1d - Same as 1a but for the month of October.

Figure 2a - The diurnal curves of standard deviation in TEC for the month of January at four stations in 1969 and three stations in 1975.

Figure 2b - Same as 2a but for the month of April.

Figure 2c - Same as 2a but for the month of July.

Figure 2d - Same as 2a but for the month of October.

Figure 3a - Comparison in TEC for January 1969 at Hamilton, Massachusetts of the observed mean, standard deviation, r.m.s. error of a 3-hour time cell, and error growth in time using an adapted prediction up to 3 hours after a reference time.

Figure 3b - Similar to 3a but using a model prediction of mean TEC. The error growth in time using the adapted prediction is shown for 12 hours after the reference time.

Figure 4a - TEC on a magnetically disturbed day, compared to the observed TEC for the day with the mean and the adapted predictions for the day using a 30-minute and a 3-hour time cell.

Figure 4b - The residual error in TEC using the predictions of 4a for the day.

Figure 5a - The diurnal curves in TEC for January 1969 from four stations comparing the mean standard deviation and the residual error using the adapted predictions with 15-minute, 1-hour and 3-hour time cells.

Figure 5b - Comparing the residual error using the indicated space-time cells to the standard deviation of the stations of figure 5a. The arrows indicate the direction of reference to applied correction.

Figure 6a - Same as 5a but for April 1969.

Figure 6b - Same as 5b but for April 1969

Figure 7a - Same as 5a but for July 1969.

Figure 7b - Same as 5b but for July 1969.

Figure 8a - Same as 5a but for October 1969.

Figure 8b - Same as 5b but for October 1969.

Figure 9a - Same as 5a but for three stations in January 1975.

Figure 9b - Same as 5b but for three stations in January 1975.

Figure 10a - Same as 9a but for April 1975.

Figure 10b - Same as 9b but for April 1975.

Figure 11a - Same as 9a but for July 1975.

Figure 11b - Same as 9b but for July 1975.

Figure 12a - Same as 9a but for October 1975.

Figure 12b - Same as 9b but for October 1975.

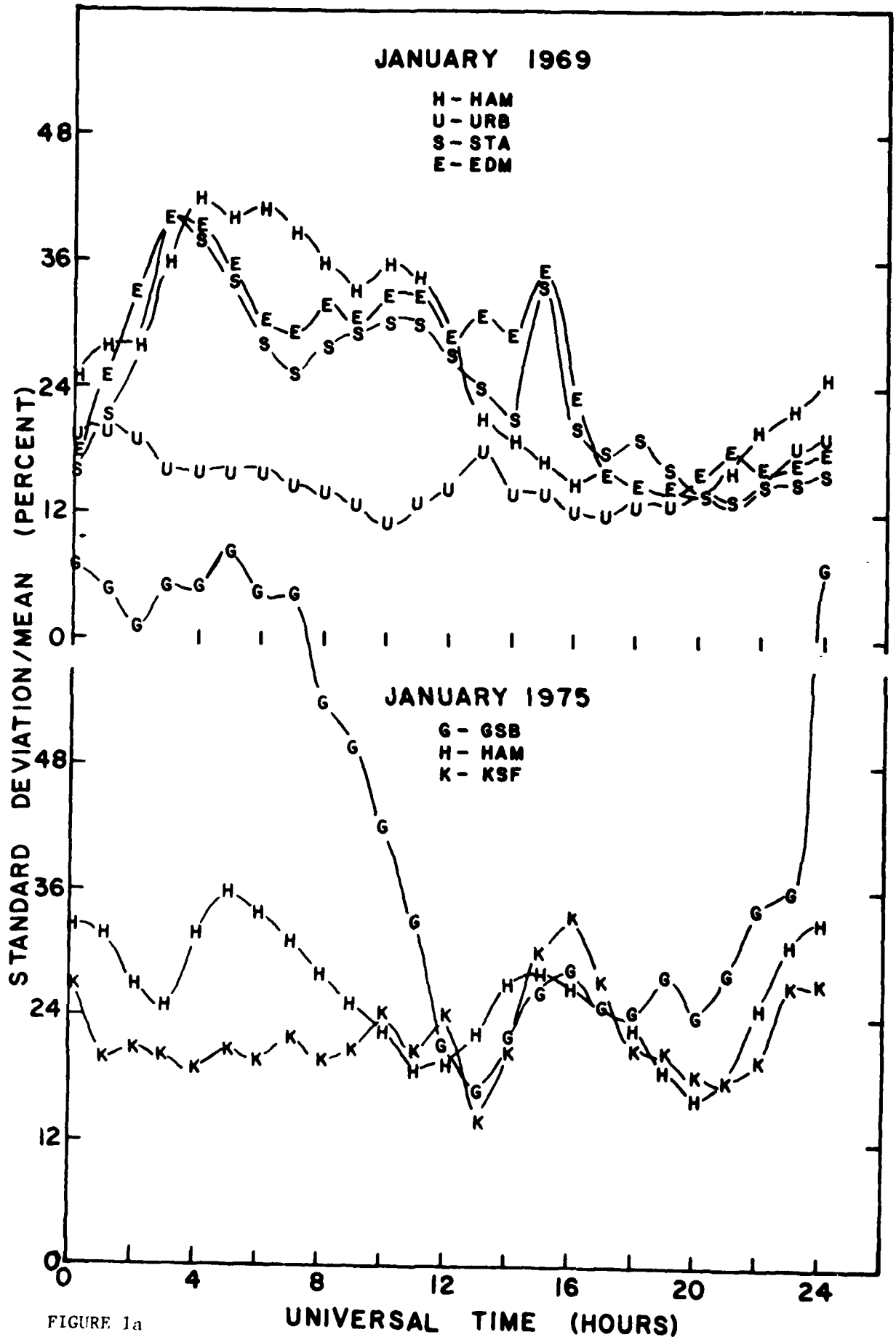
JANUARY 1969
H - HAM
U - URB
S - STA
E - EDM
JANUARY 1975
G - GSB
H - HAM
K - KSF
STANDARD DEVIATION/MEAN (PERCENT)
UNIVERSAL TIME (HOURS)
0
12
24
36
48
4
8
16
20

FIGURE 1a

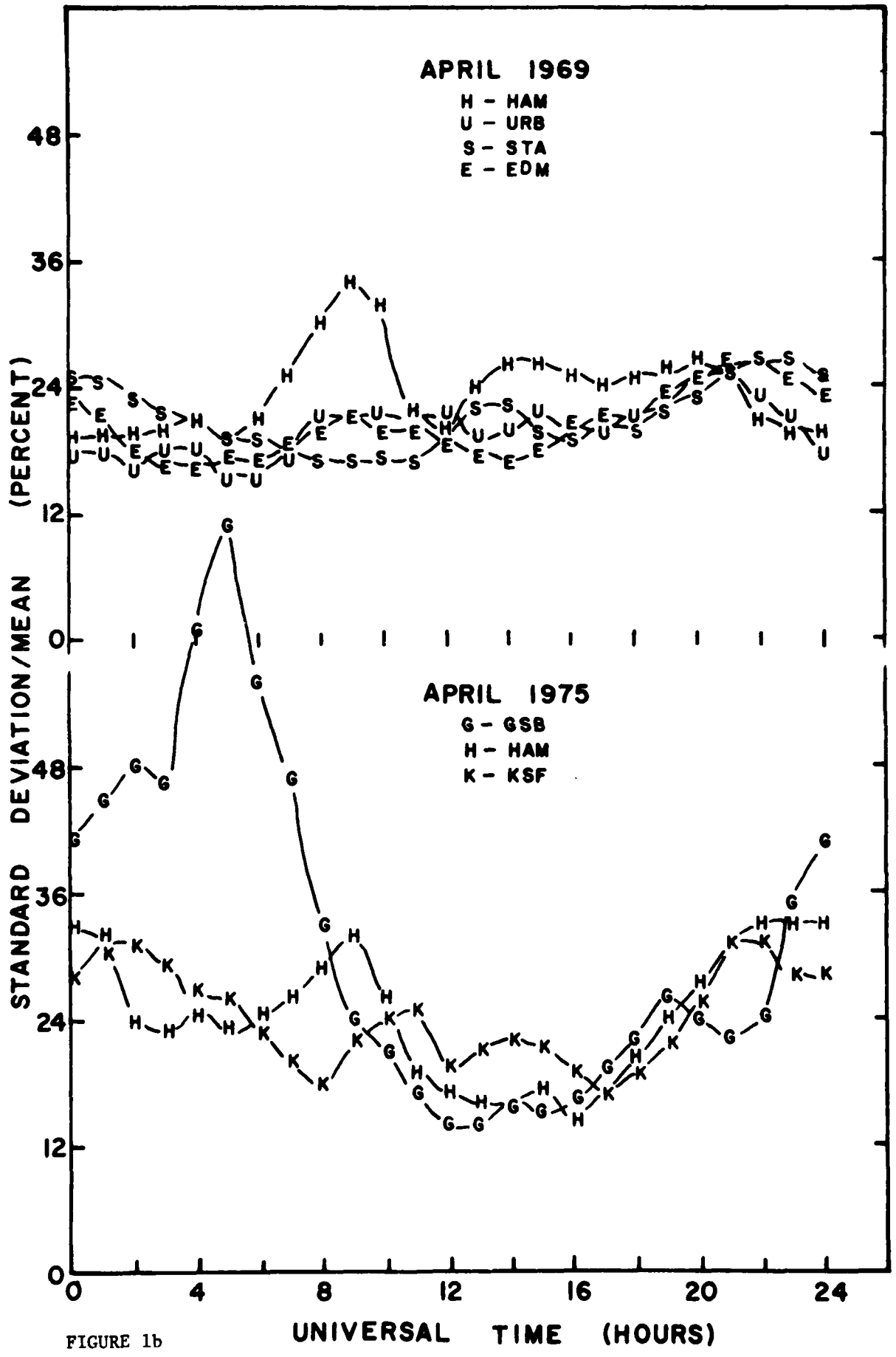
APRIL 1969
H - HAM
U - URB
S - STA
E - EDM
APRIL 1975
G - GSB
H - HAM
K - KSF
STANDARD DEVIATION/MEAN (PERCENT)
UNIVERSAL TIME (HOURS)
0
12
24
36
48
0
4
8
12
16
20
24

FIGURE 1b

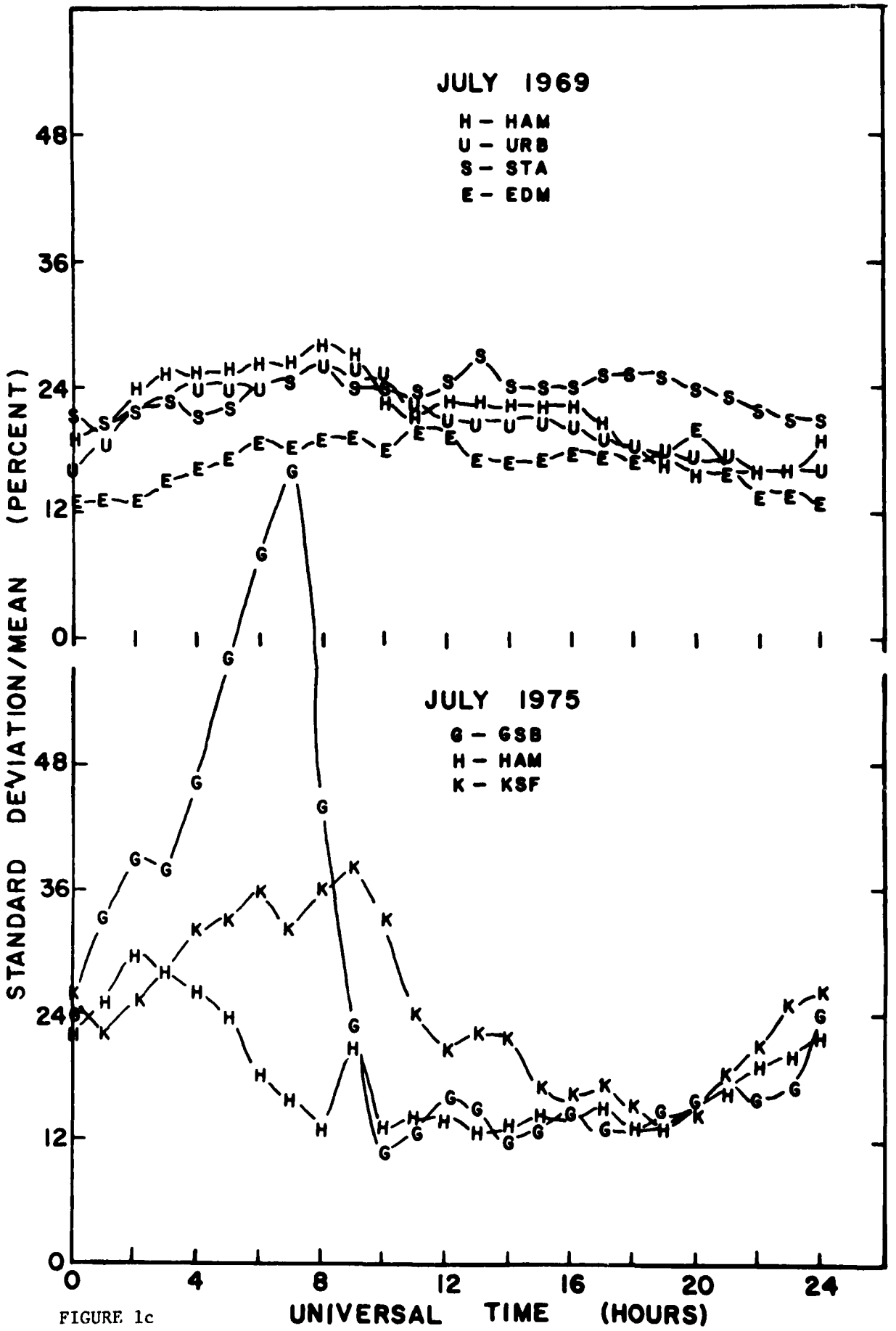
JULY 1969
H – HAM
U – URB
S – STA
E – EDM
JULY 1975
G – GSB
H – HAM
K – KSF
STANDARD DEVIATION/MEAN (PERCENT)
0
12
24
36
48
0
4
8
12
16
20
24
UNIVERSAL TIME (HOURS)

FIGURE 1c

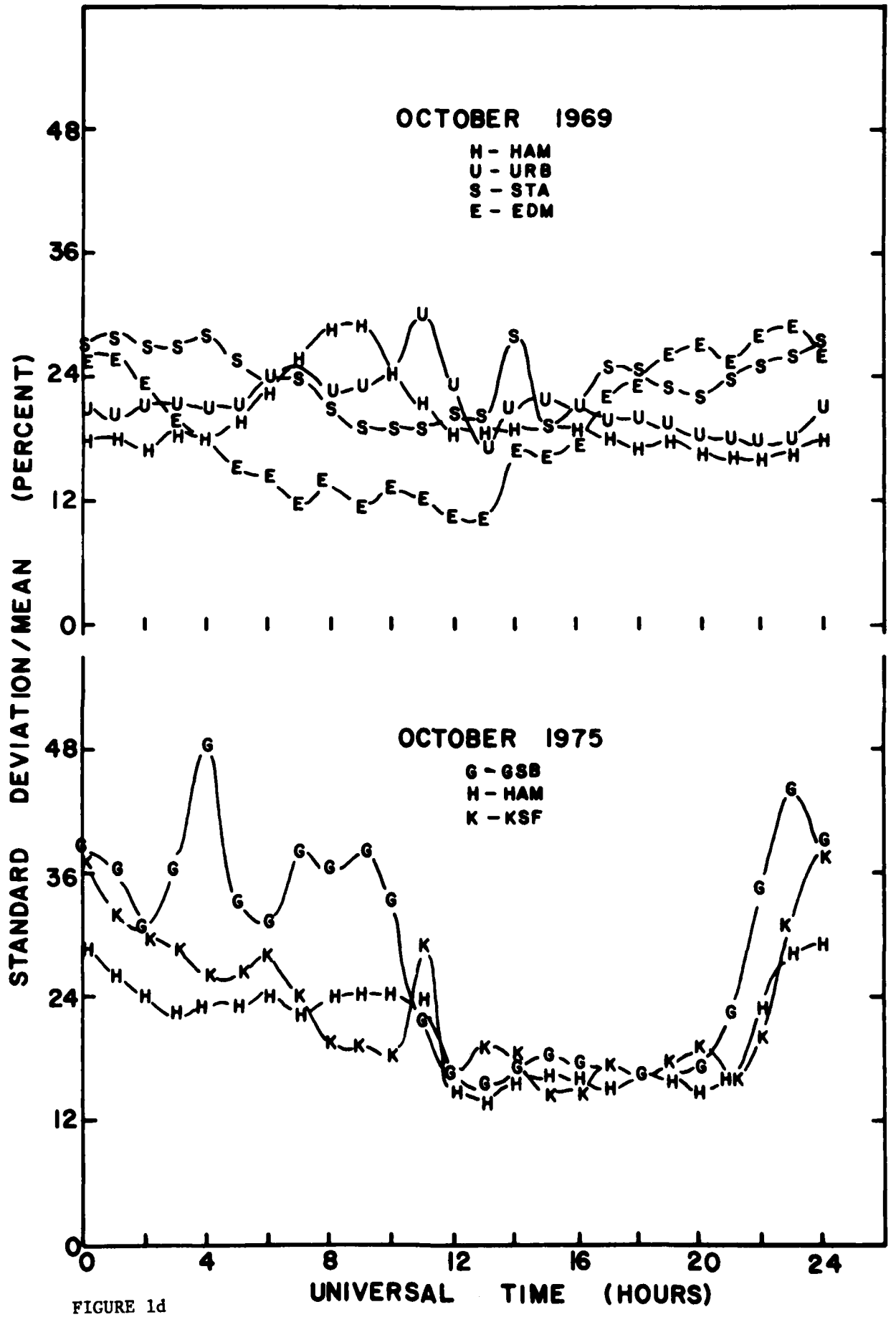
OCTOBER 1969
H - HAM
U - URB
S - STA
E - EDM
OCTOBER 1975
G - GSB
H - HAM
K - KSF
STANDARD DEVIATION/MEAN (PERCENT)
UNIVERSAL TIME (HOURS)
0
12
24
36
48
0
4
8
12
16
20
24

FIGURE 1d

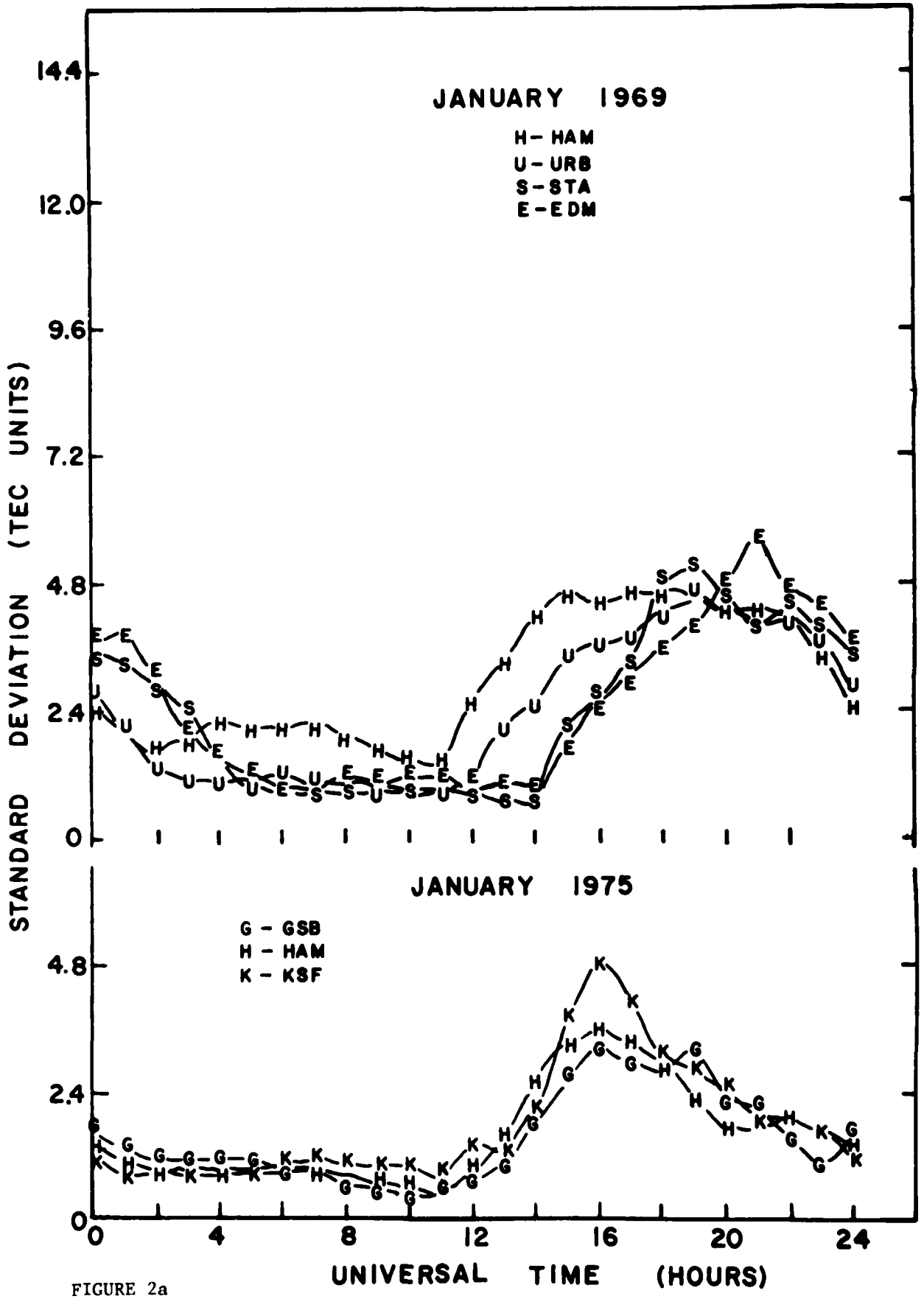
JANUARY 1969
H - HAM
U - URB
S - STA
E - EDM
JANUARY 1975
G - GSB
H - HAM
K - KSF
STANDARD DEVIATION (TEC UNITS)
UNIVERSAL TIME (HOURS)
14.4
12.0
9.6
7.2
4.8
2.4
0
0
4
8
12
16
20
24

FIGURE 2a

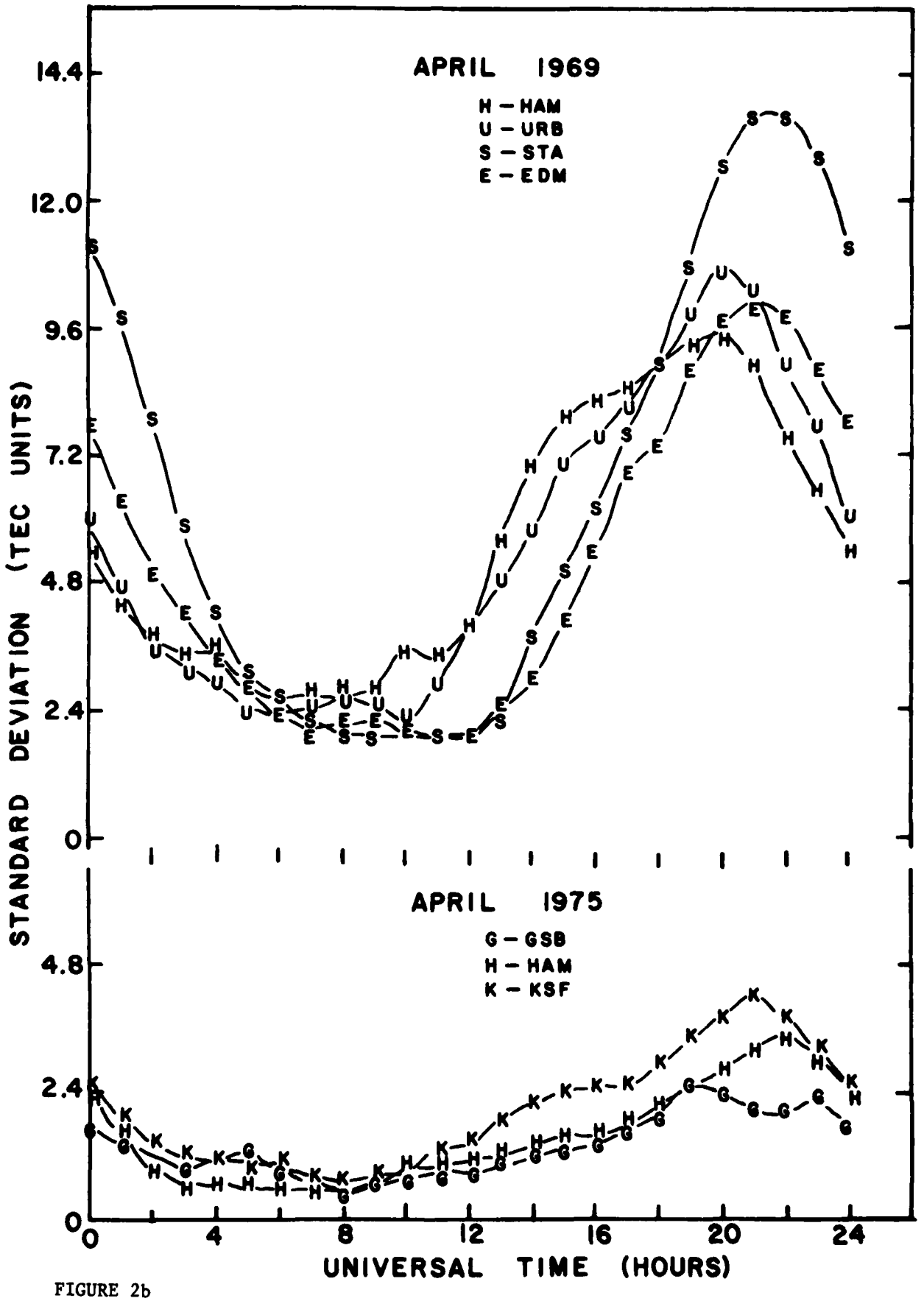
APRIL 1969
H – HAM
U – URB
S – STA
E – EDM
STANDARD DEVIATION (TEC UNITS)
14.4
12.0
9.6
7.2
4.8
2.4
0
APRIL 1975
G – GSB
H – HAM
K – KSF
4.8
2.4
0
0
4
8
12
16
20
24
UNIVERSAL TIME (HOURS)

FIGURE 2b

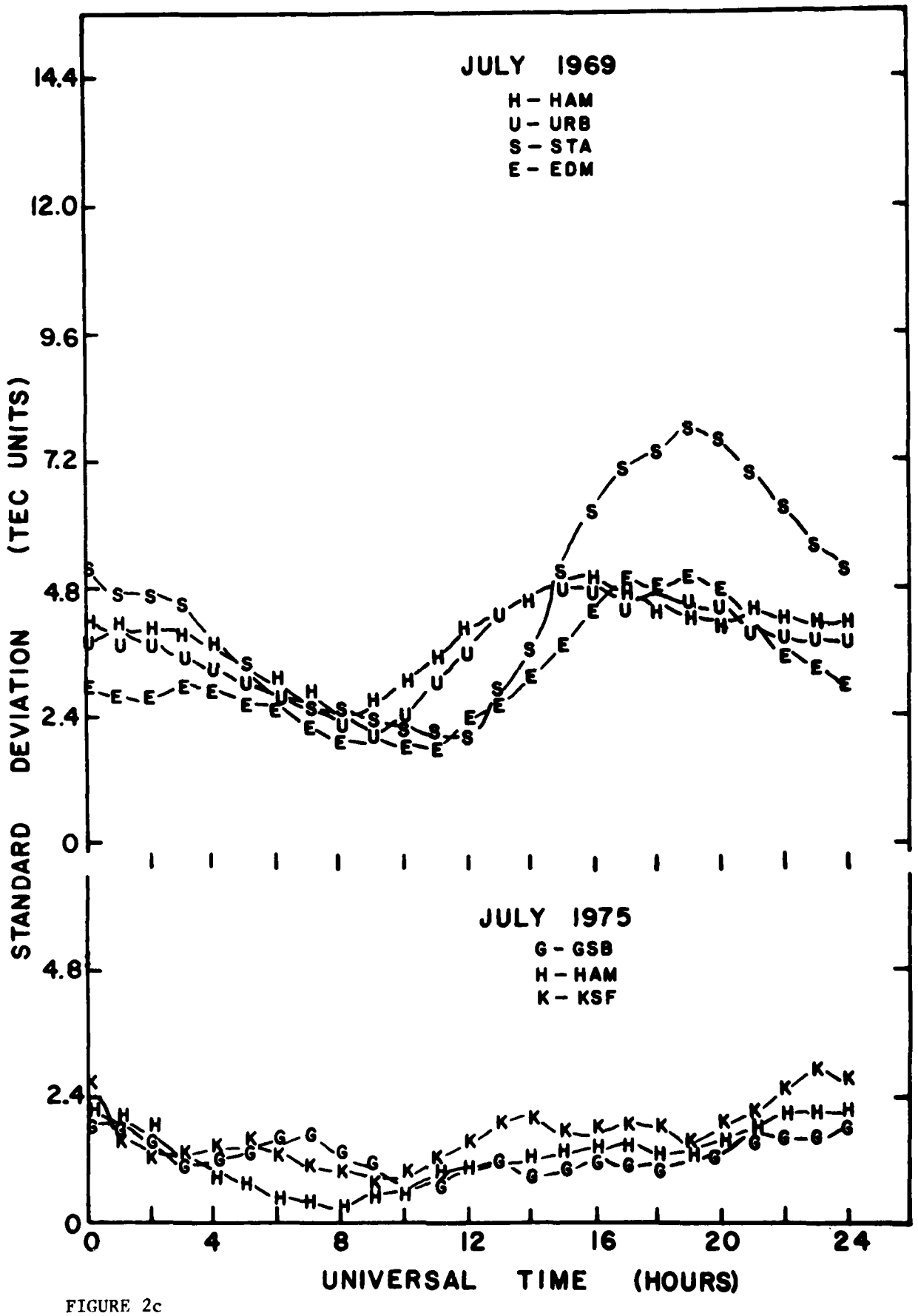
JULY 1969
H - HAM
U - URB
S - STA
E - EDM
14.4
12.0
9.6
7.2
4.8
2.4
0
STANDARD DEVIATION (TEC UNITS)
JULY 1975
G - GSB
H - HAM
K - KSF
4.8
2.4
0
0
4
8
12
16
20
24
UNIVERSAL TIME (HOURS)

FIGURE 2c

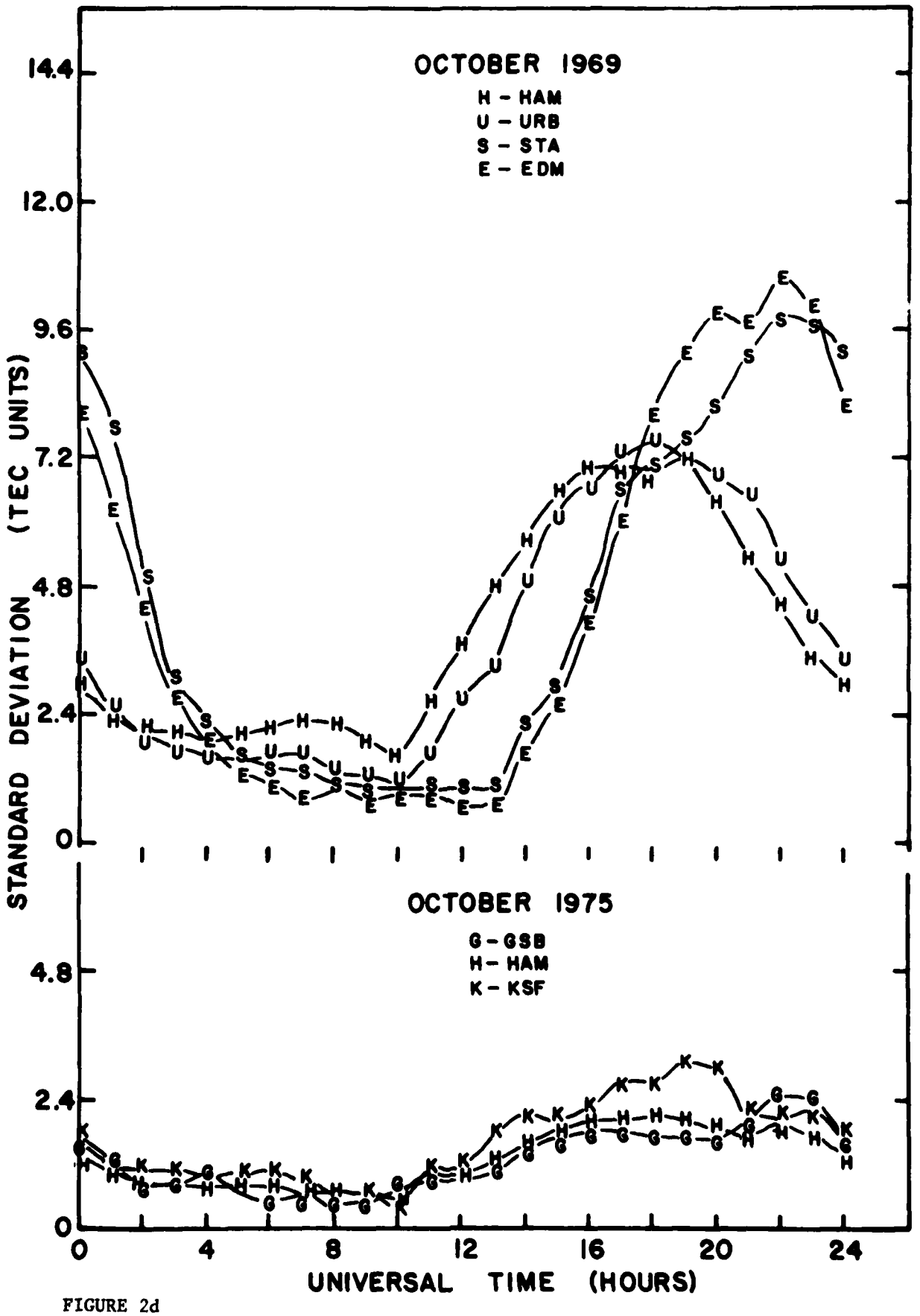
OCTOBER 1969
H - HAM
U - URB
S - STA
E - EDM
14.4
12.0
9.6
7.2
4.8
2.4
0
STANDARD DEVIATION (TEC UNITS)
OCTOBER 1975
G - GSB
H - HAM
K - KSF
4.8
2.4
0
0
4
8
12
16
20
24
UNIVERSAL TIME (HOURS)

FIGURE 2d

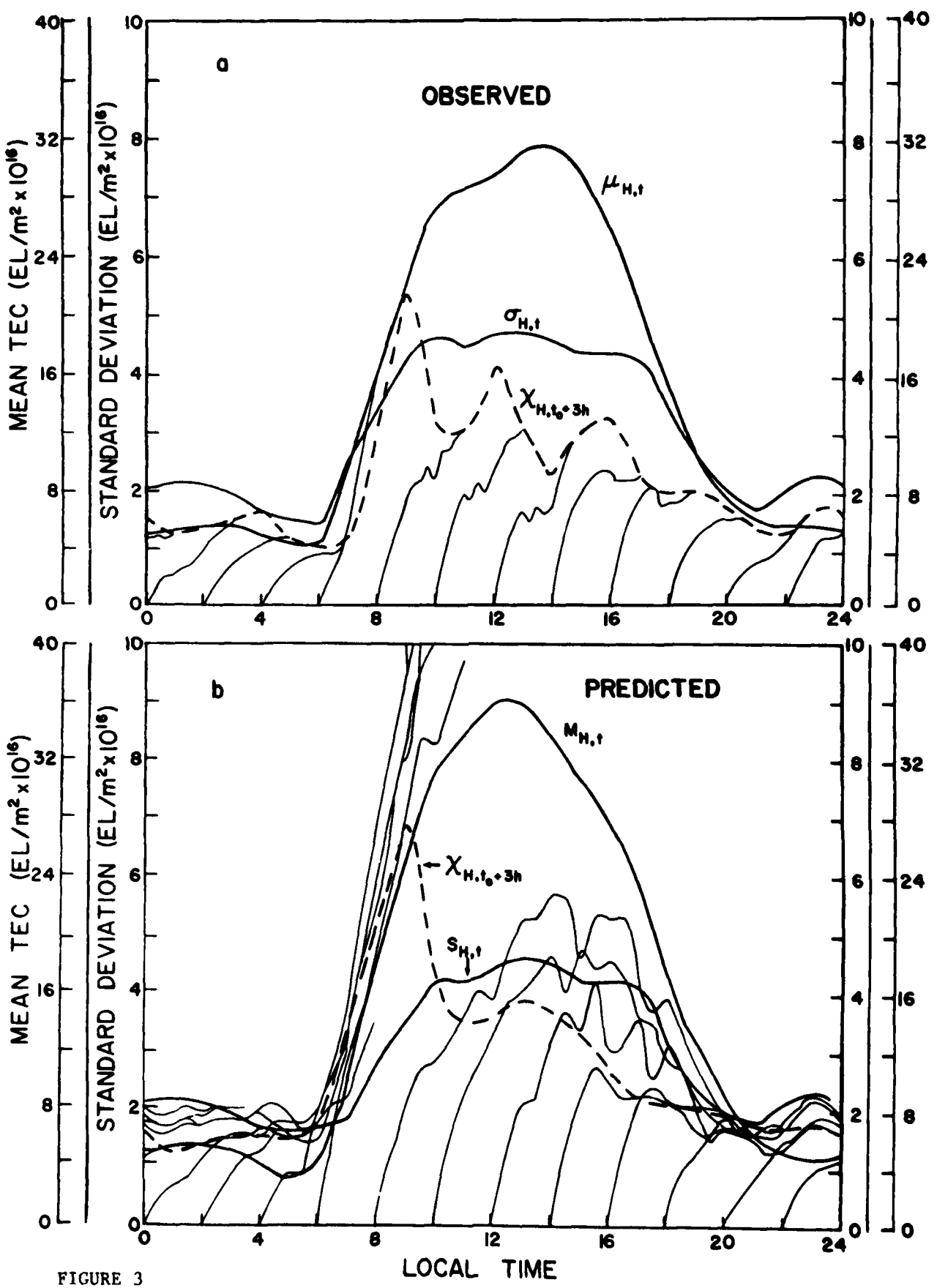
HAMILTON JANUARY 1969
a
OBSERVED
$\mu_{H,t}$
$\sigma_{H,t}$
χ_{H,t_0+3h}
b
PREDICTED
$M_{H,t}$
χ_{H,t_0+3h}
$s_{H,t}$
MEAN TEC (EL/m² x 10¹⁶)
STANDARD DEVIATION (EL/m² x 10¹⁶)
LOCAL TIME
0
4
8
12
16
20
24
0
2
4
6
8
10
16
24
32
40

FIGURE 3

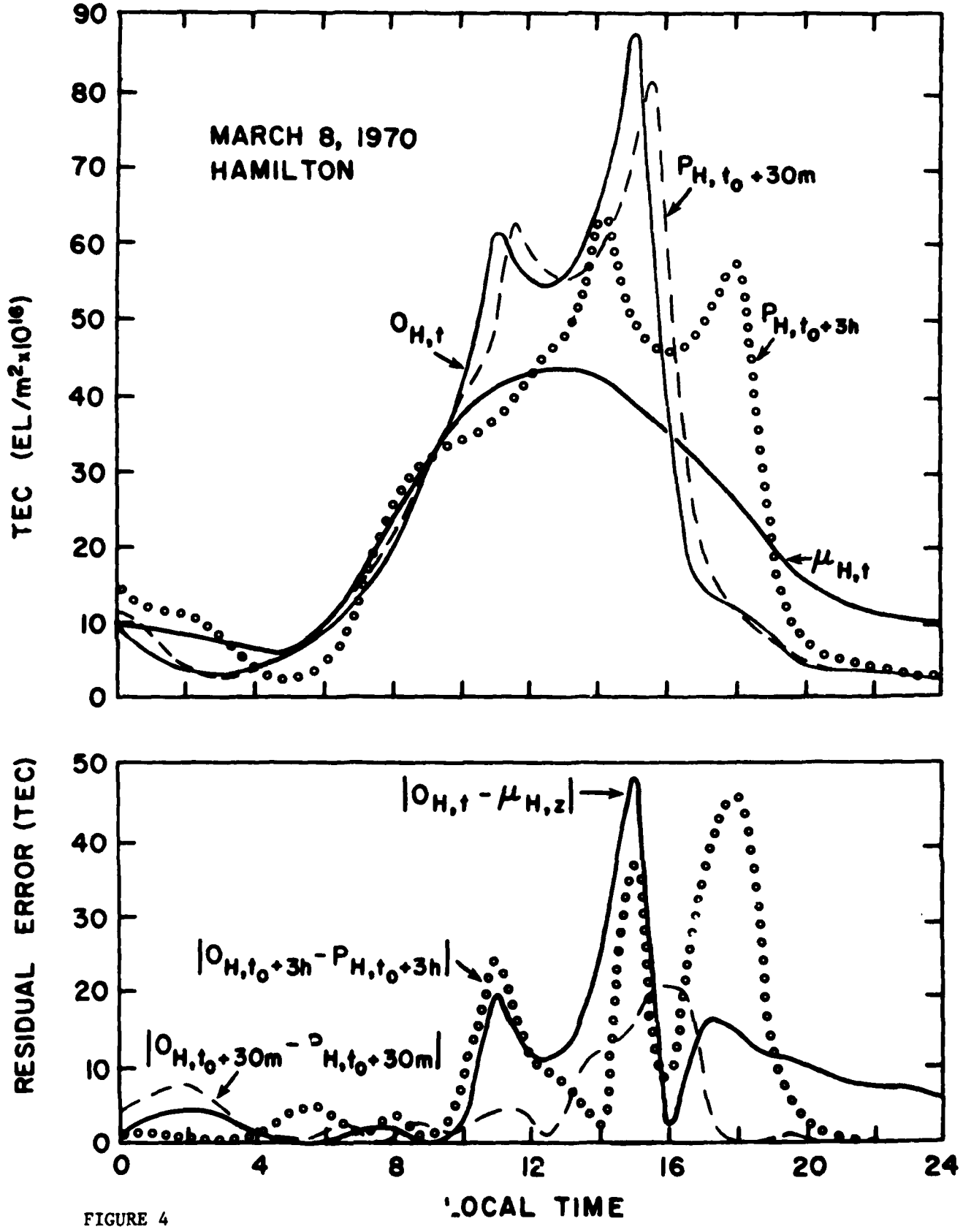
MARCH 8, 1970
HAMILTON
TEC (EL/m²x10¹⁶)
P_{H,t_0+30m}
$O_{H,t}$
P_{H,t_0+3h}
$\mu_{H,t}$
RESIDUAL ERROR (TEC)
$|O_{H,t} - \mu_{H,z}|$
$|O_{H,t_0+3h} - P_{H,t_0+3h}|$
$|O_{H,t_0+30m} - P_{H,t_0+30m}|$
LOCAL TIME

FIGURE 4

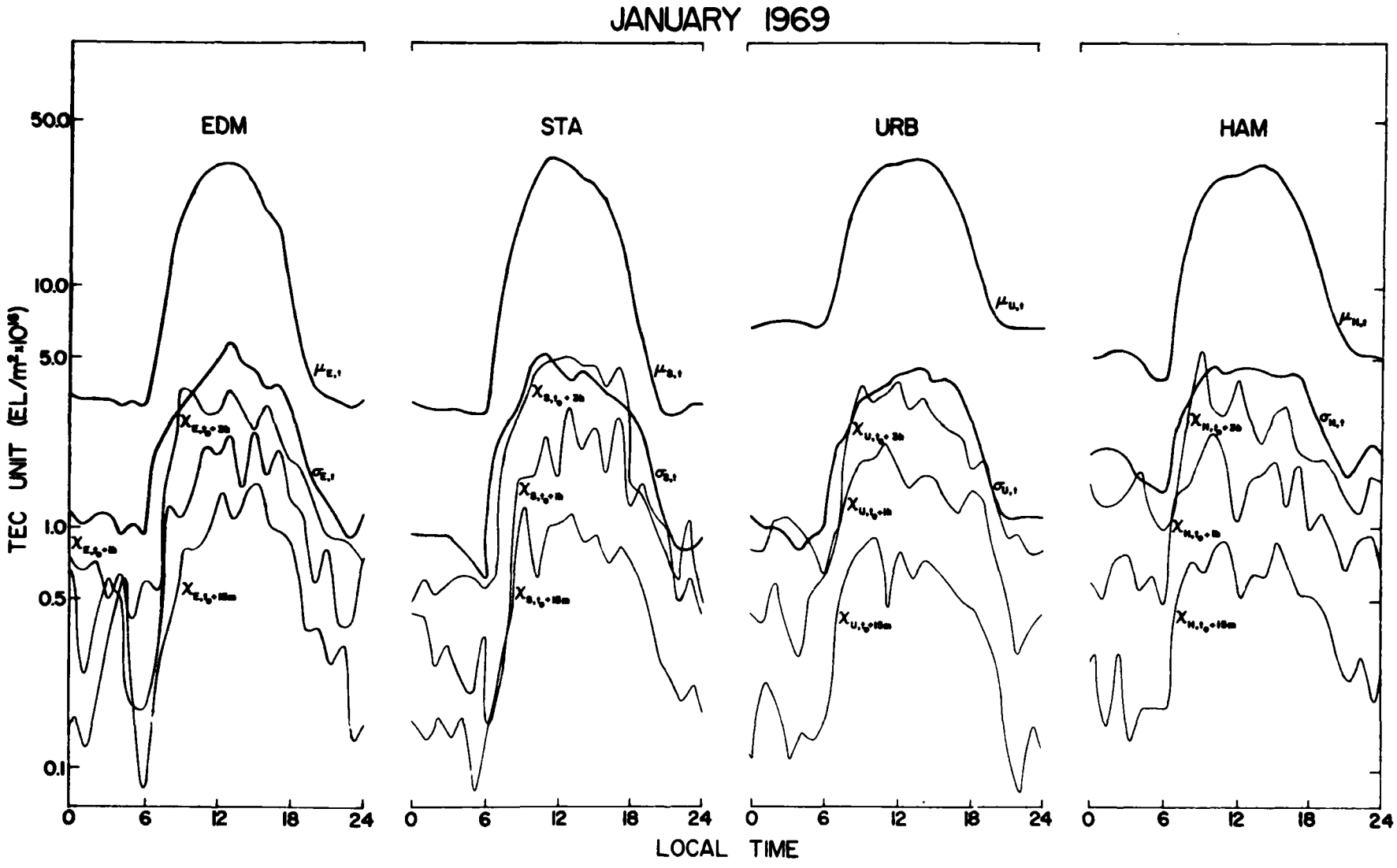
JANUARY 1969
EDM
STA
URB
HAM
50.0
10.0
5.0
1.0
0.5
0.1
TEC UNIT (EL/m²x10¹⁶)
0
6
12
18
24
LOCAL TIME

FIGURE 5a

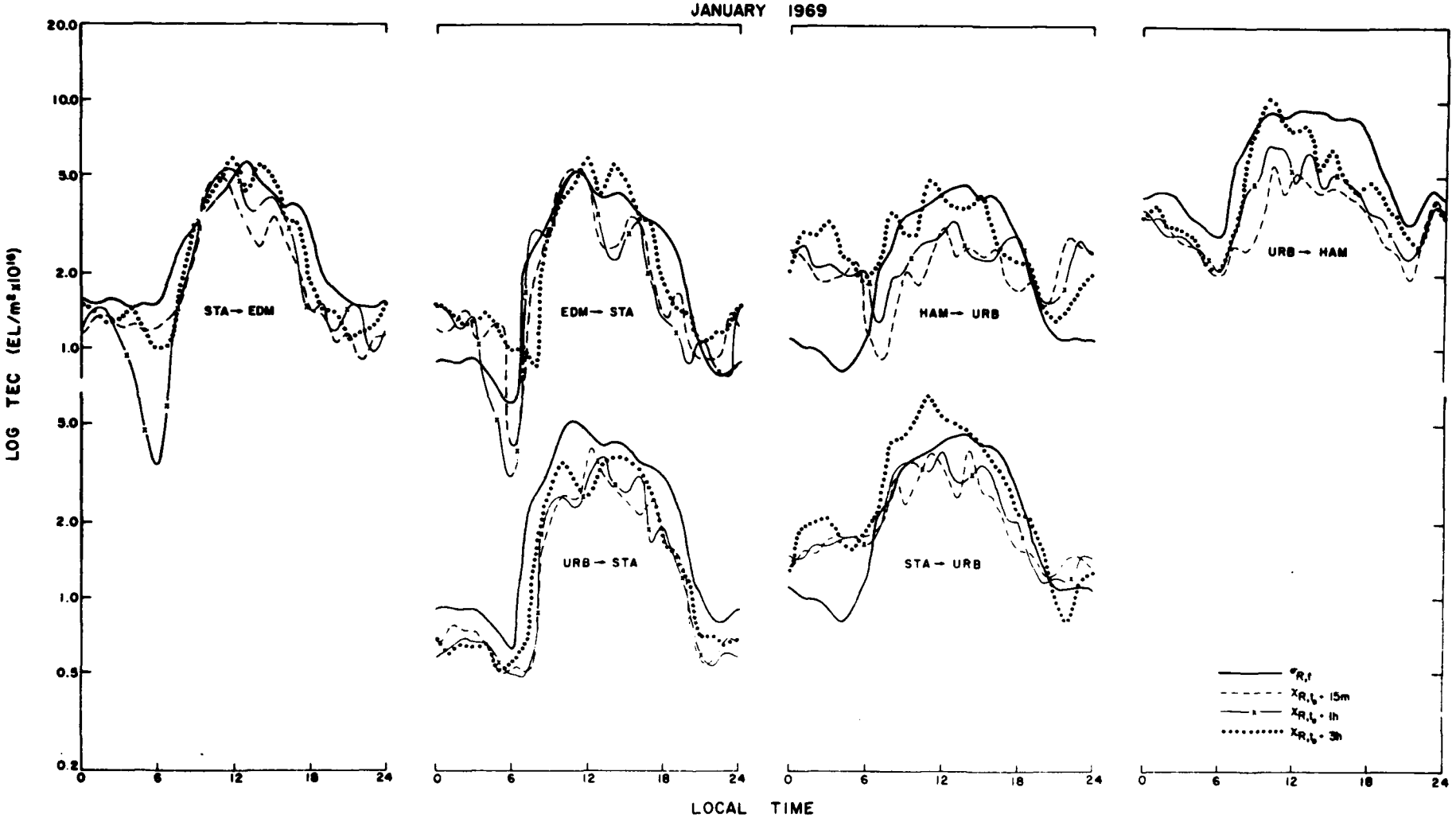
JANUARY 1969
LOG TEC (EL/m²x10¹⁶)
20.0
10.0
5.0
2.0
1.0
0.5
0.2
STA→ EDM
EDM→ STA
HAM→ URB
URB→ HAM
URB→ STA
STA→ URB
0
6
12
18
24
LOCAL TIME
$\sigma_{R,t}$
χ_{R,t_0} - 15m
χ_{R,t_0} - 1h
χ_{R,t_0} - 3h

FIGURE 5b

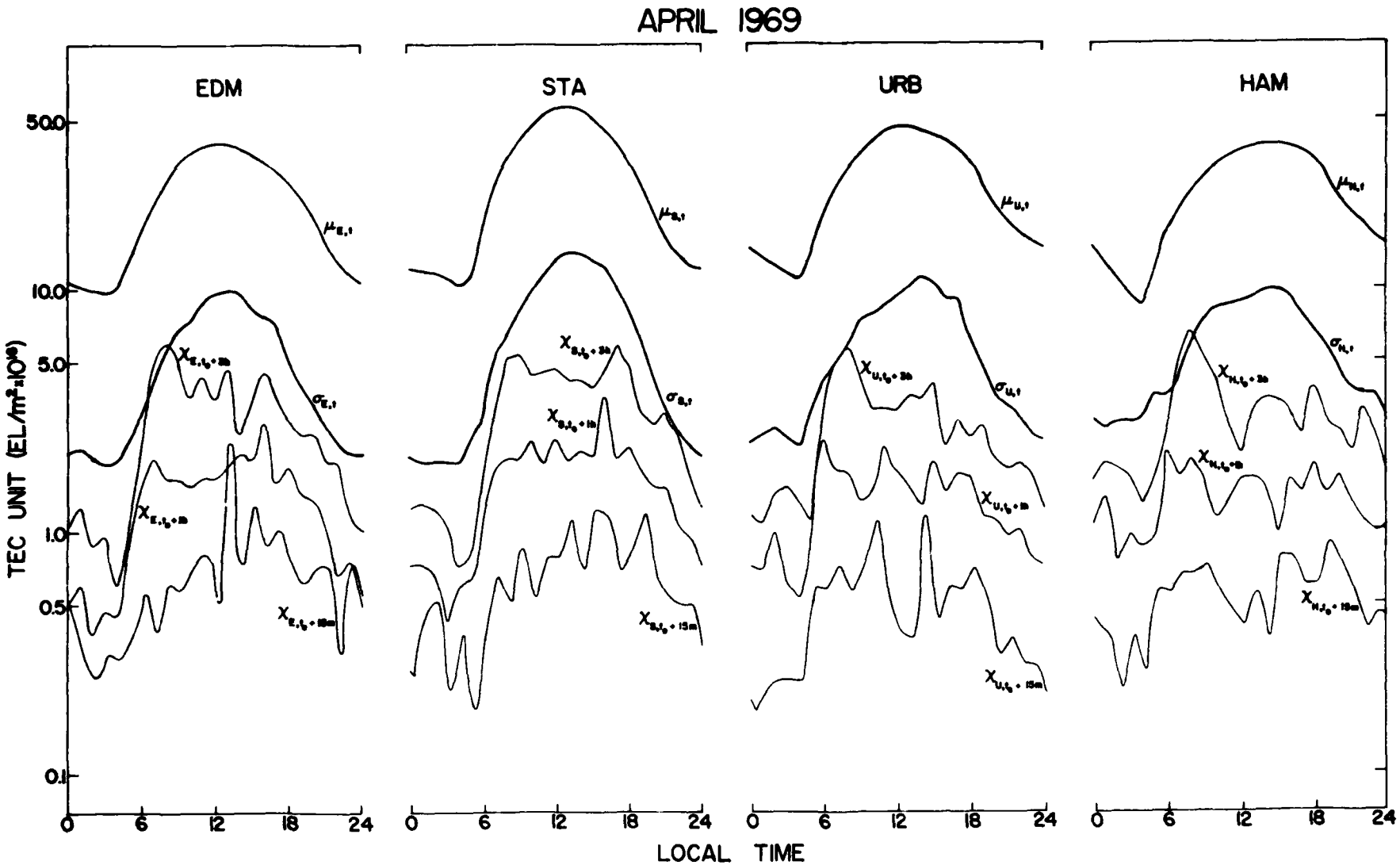
APRIL 1969
EDM
STA
URB
HAM
50.0
10.0
5.0
1.0
0.5
0.1
TEC UNIT (EL/m²x10¹⁶)
0
6
12
18
24
LOCAL TIME

FIGURE 6a

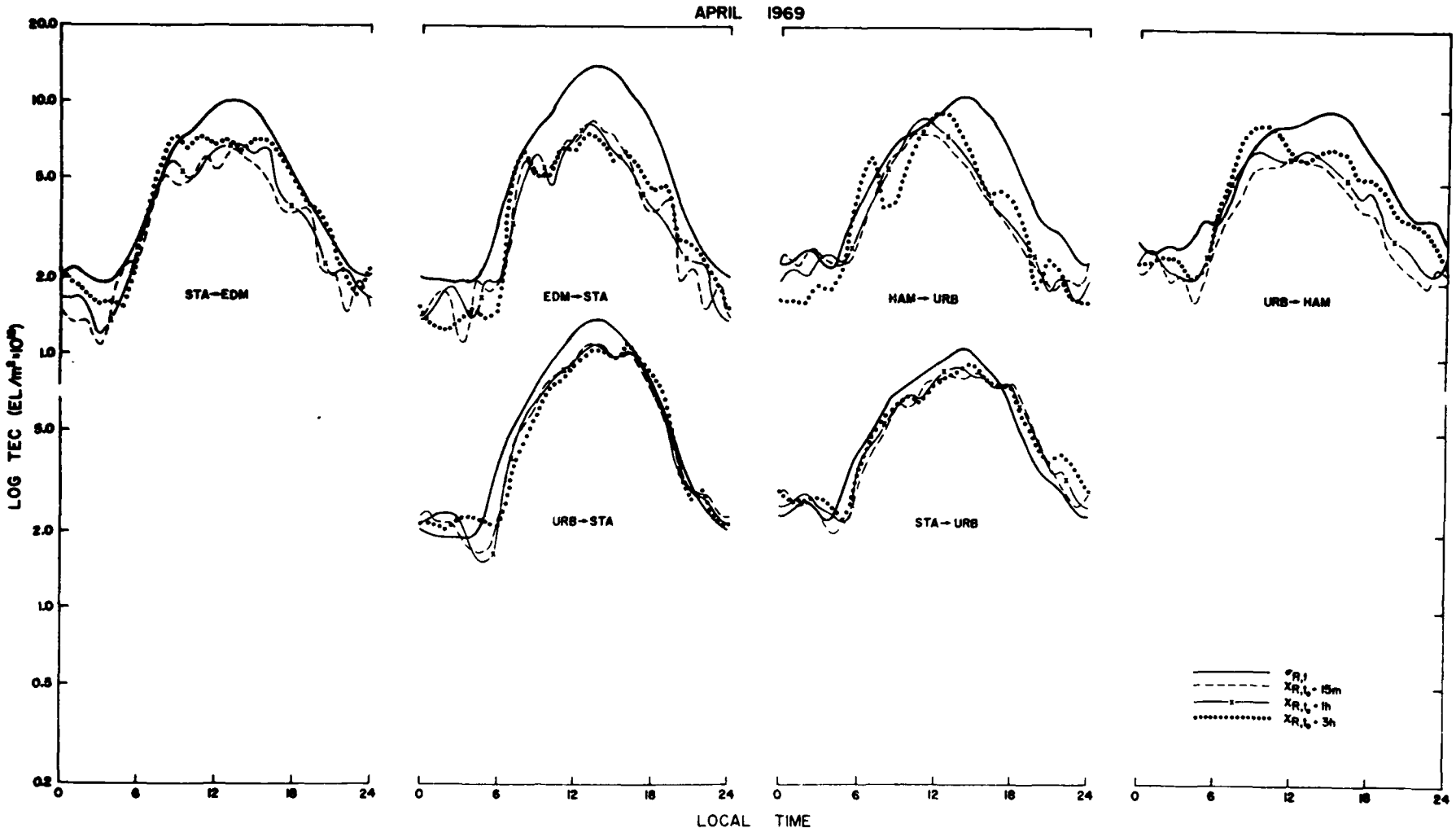
APRIL 1969
STA—EDM
EDM—STA
HAM—URB
URB—HAM
URB—STA
STA—URB
LOG TEC (EL/m²·10¹⁶)
20.0
10.0
5.0
2.0
1.0
0.5
0.2
0
6
12
18
24
LOCAL TIME
$\sigma_{R,t}$
χ_{R,t_b} = 15m
χ_{R,t_b} = 1h
χ_{R,t_b} = 3h

FIGURE 6b

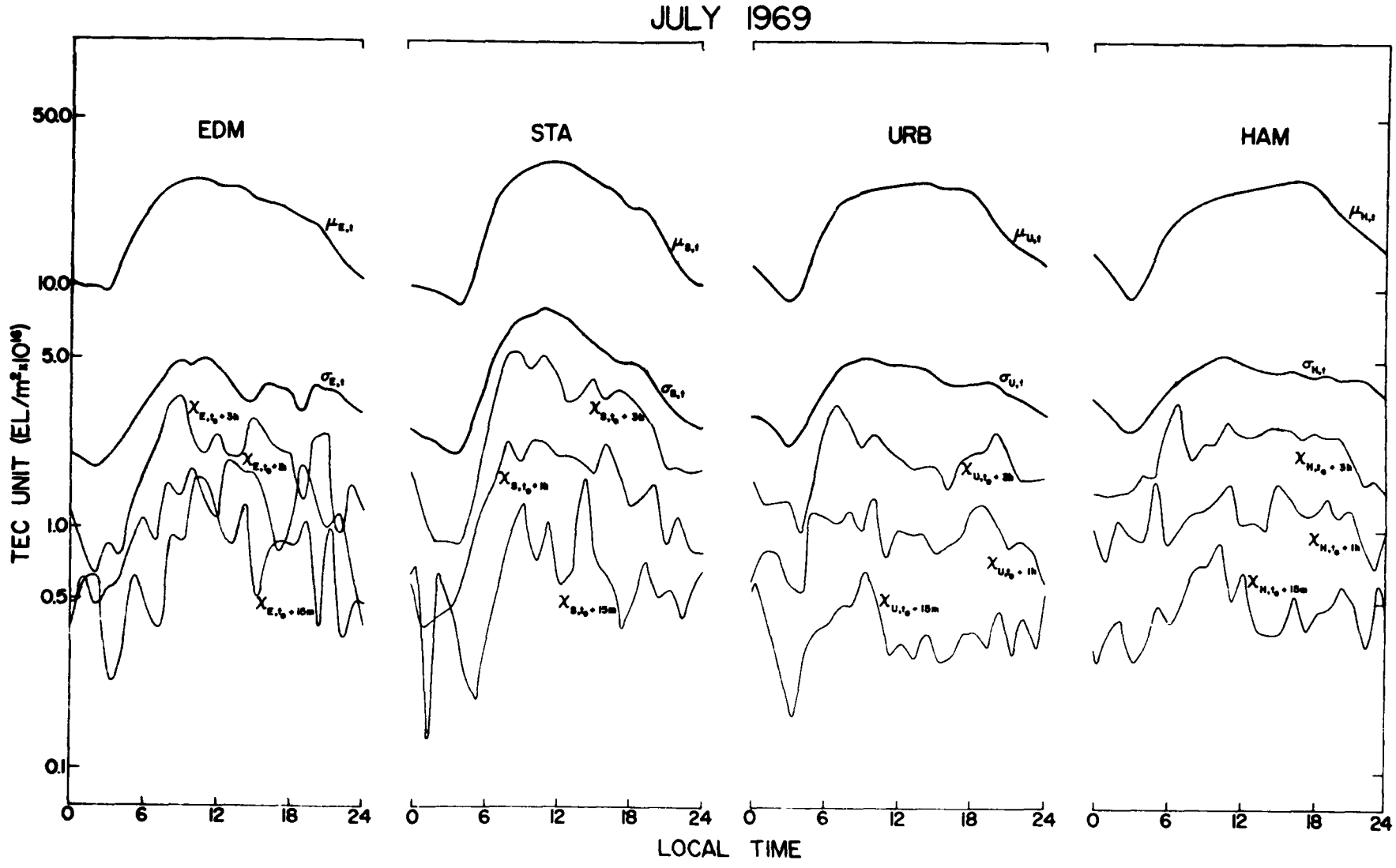
JULY 1969
EDM
STA
URB
HAM
50.0
10.0
5.0
1.0
0.5
0.1
TEC UNIT (EL/m²x10¹⁶)
0
6
12
18
24
LOCAL TIME

FIGURE 7a

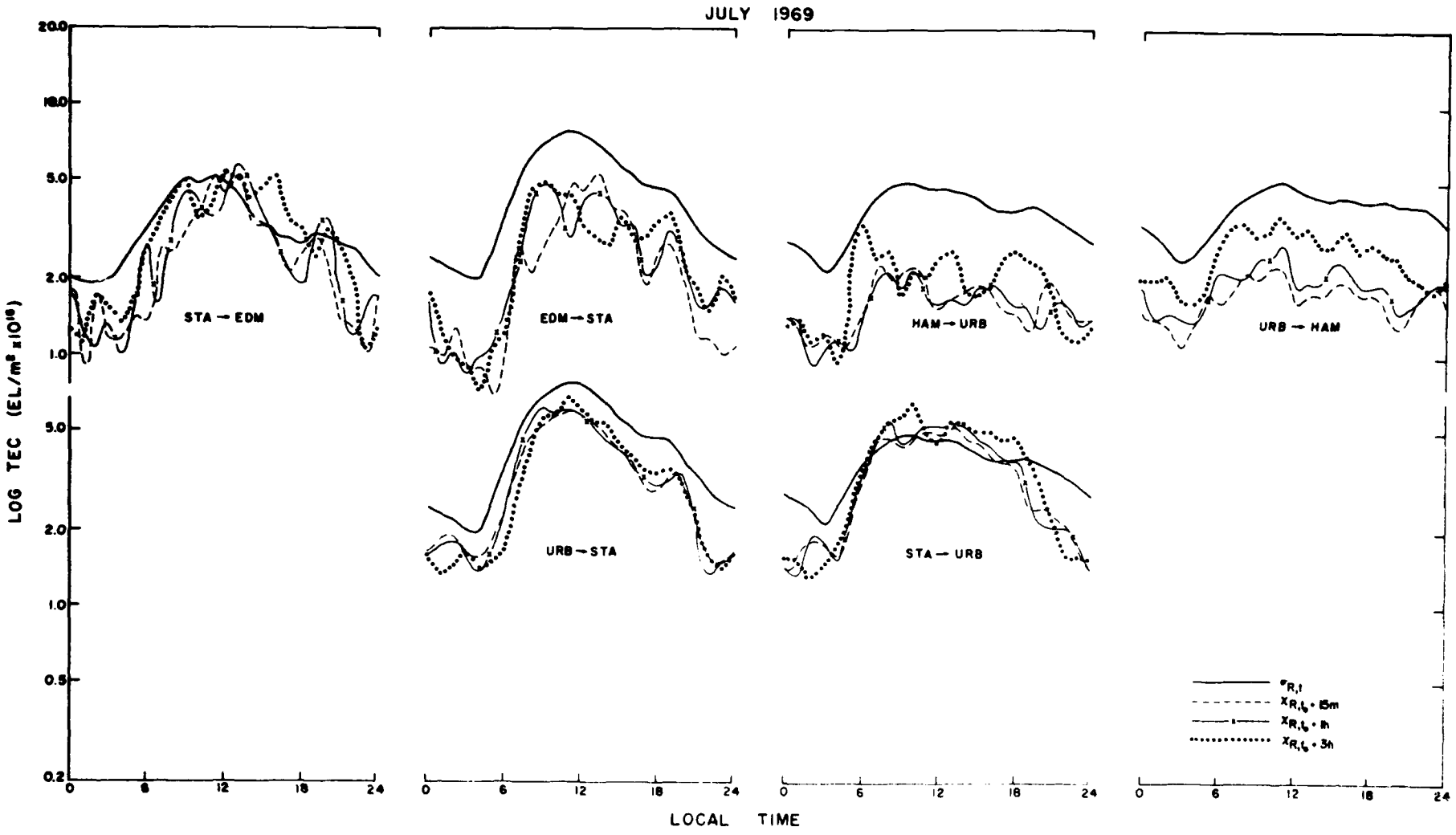
JULY 1969
LOG TEC (EL/m³ x10¹⁶)
20.0
10.0
5.0
2.0
1.0
5.0
2.0
1.0
0.5
0.2
STA — EDM
EDM — STA
HAM — URB
URB — HAM
URB — STA
STA — URB
0
6
12
18
24
LOCAL TIME
$\sigma_{R,t}$
$\chi_{R,t}$ • 15m
$\chi_{R,t}$ • 1h
$\chi_{R,t}$ • 3h

FIGURE 7b

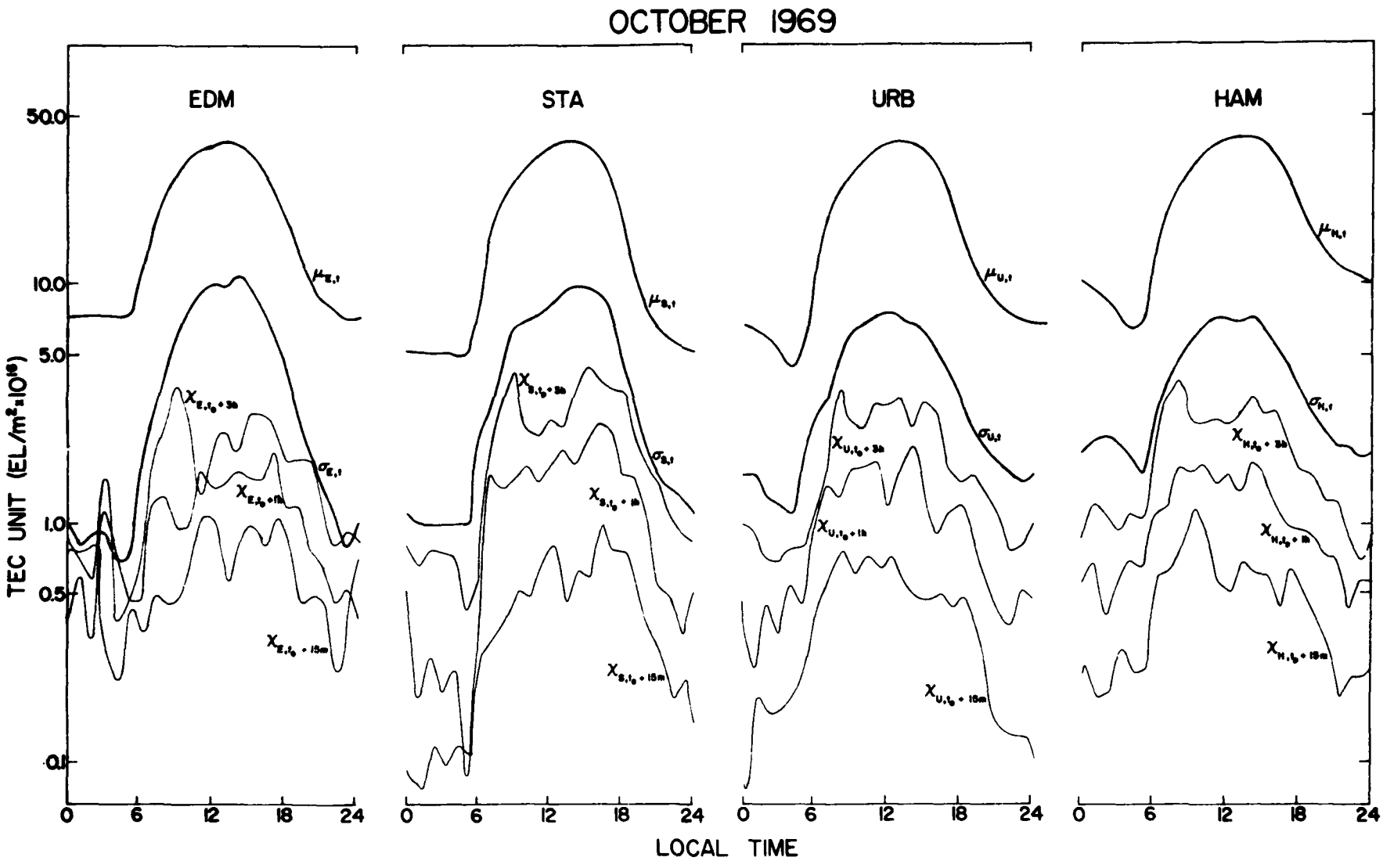
OCTOBER 1969
EDM
STA
URB
HAM
50.0
10.0
5.0
1.0
0.5
0.1
TEC UNIT (EL/m²x10¹⁶)
0
6
12
18
24
LOCAL TIME

FIGURE 8a

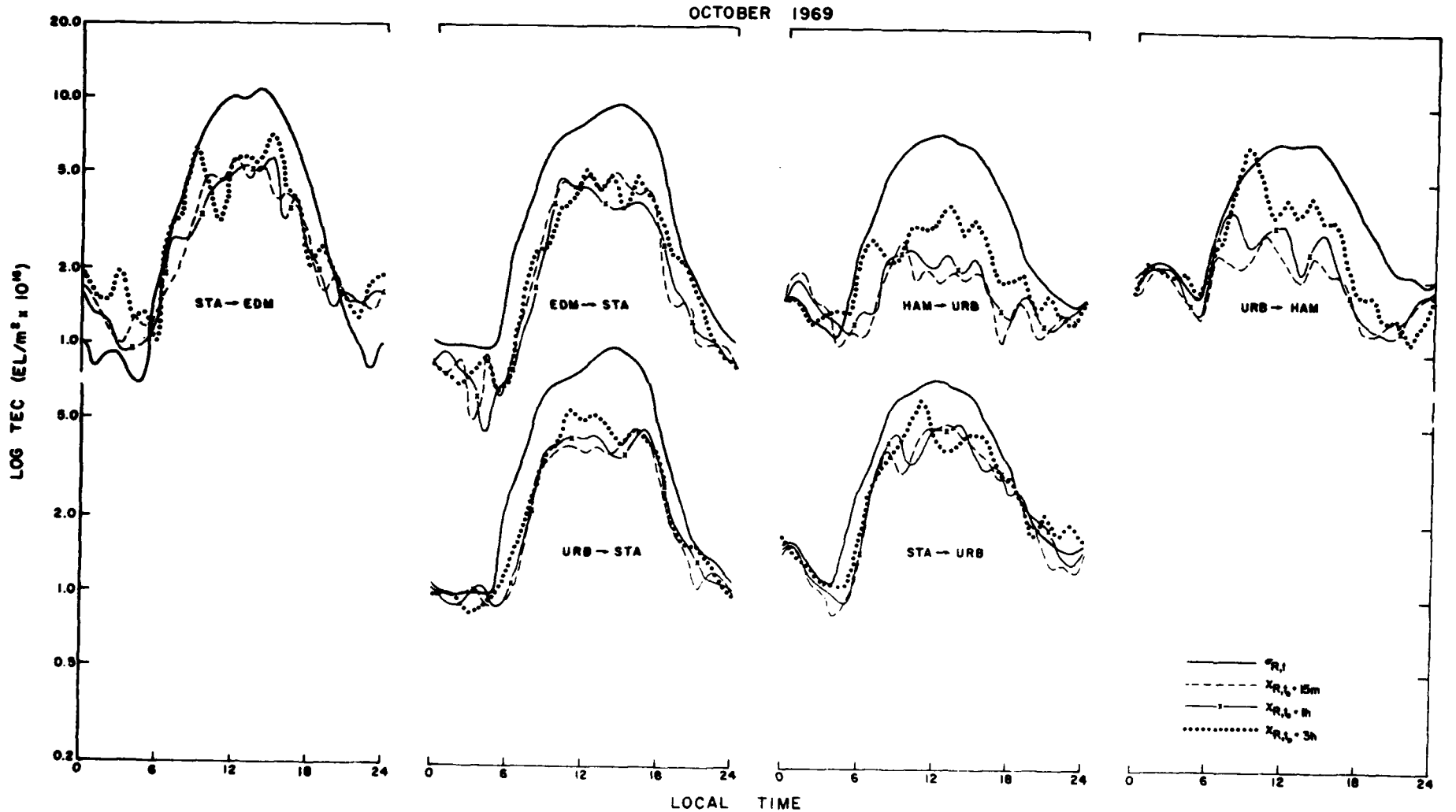
OCTOBER 1969
LOG TEC (EL/m² x 10¹⁶)
20.0
10.0
5.0
2.0
1.0
0.5
0.2
STA — EDM
EDM — STA
HAM — URB
URB — HAM
URB — STA
STA — URB
0
6
12
18
24
LOCAL TIME
$\sigma_{R,t}$
$\chi_{R,t}$ = 15m
$\chi_{R,t}$ = 1h
$\chi_{R,t}$ = 3h

FIGURE 8b

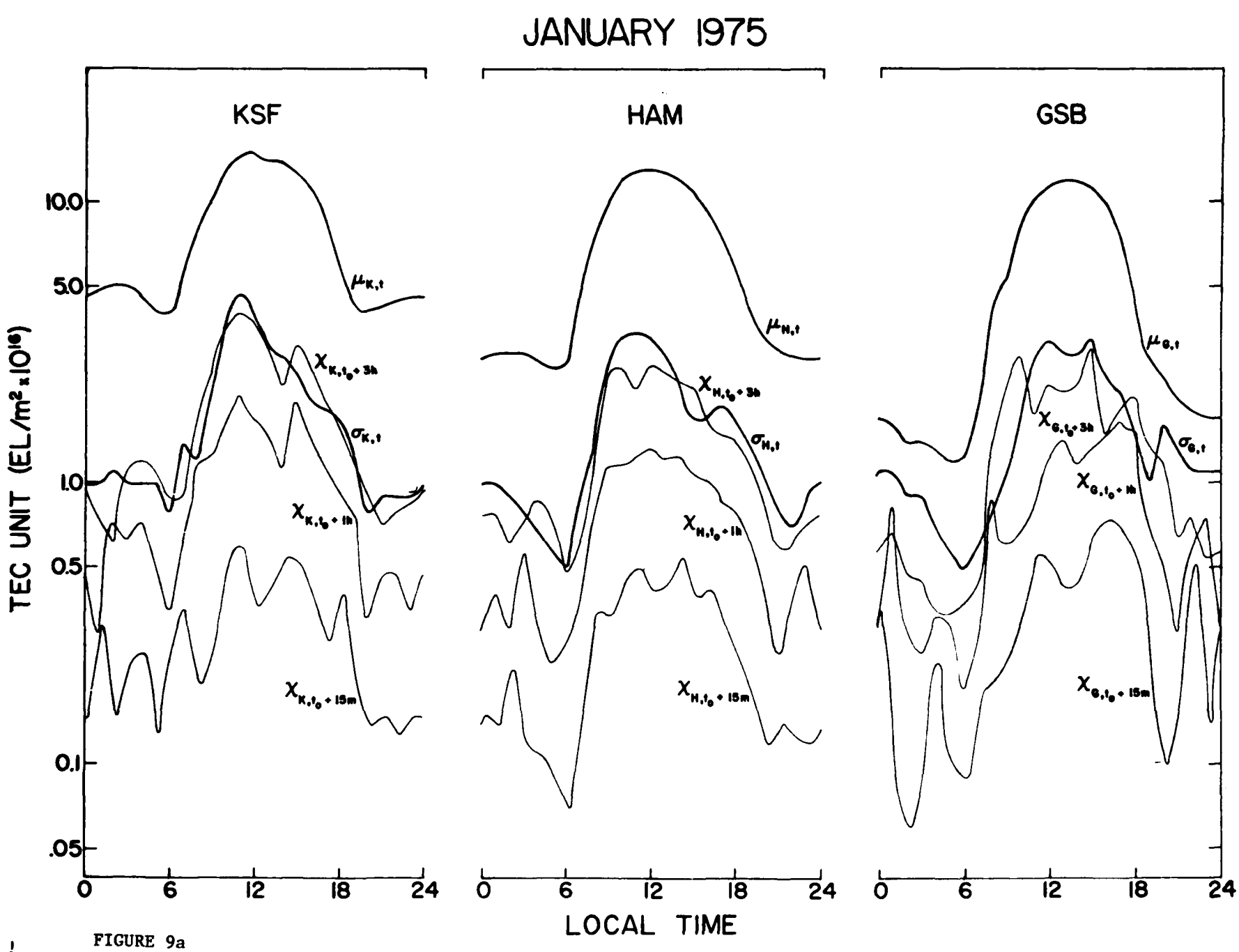
JANUARY 1975
KSF
HAM
GSB
TEC UNIT (EL/m² x 10¹⁶)
10.0
5.0
1.0
0.5
0.1
.05
$\mu_{K,t}$
χ_{K,t_0+3h}
$\sigma_{K,t}$
χ_{K,t_0+1h}
χ_{K,t_0+15m}
$\mu_{H,t}$
χ_{H,t_0+3h}
$\sigma_{H,t}$
χ_{H,t_0+1h}
χ_{H,t_0+15m}
$\mu_{G,t}$
χ_{G,t_0+3h}
$\sigma_{G,t}$
χ_{G,t_0+1h}
χ_{G,t_0+15m}
0
6
12
18
24
LOCAL TIME

FIGURE 9a

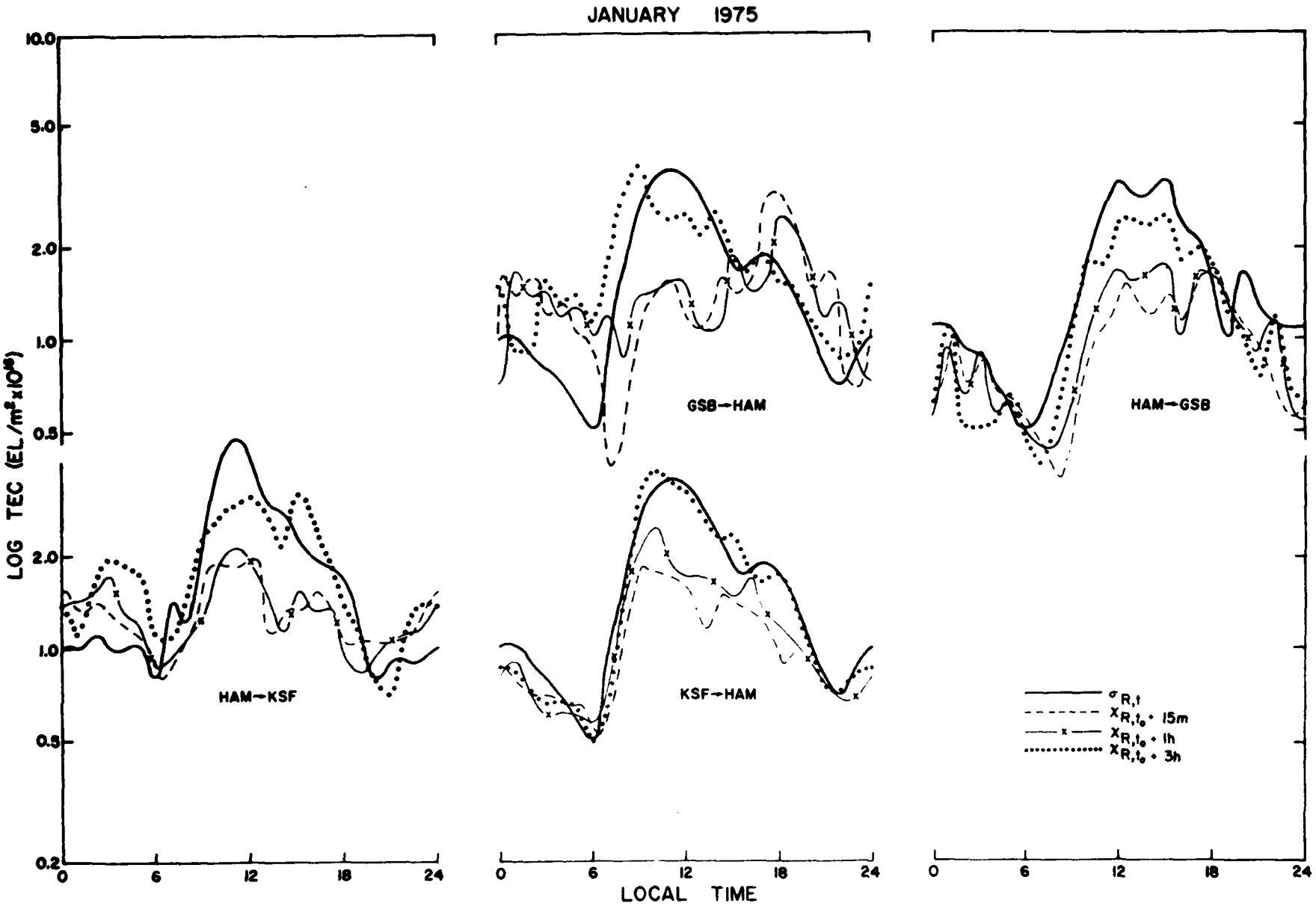
JANUARY 1975
LOG TEC (EL/m²x10¹⁶)
10.0
5.0
2.0
1.0
0.5
2.0
1.0
0.5
0.2
HAM→KSF
GSB→HAM
KSF→HAM
HAM→GSB
0
6
12
18
24
LOCAL TIME
σR,t
XR,to + 15m
XR,to + 1h
XR,to + 3h

FIGURE 9b

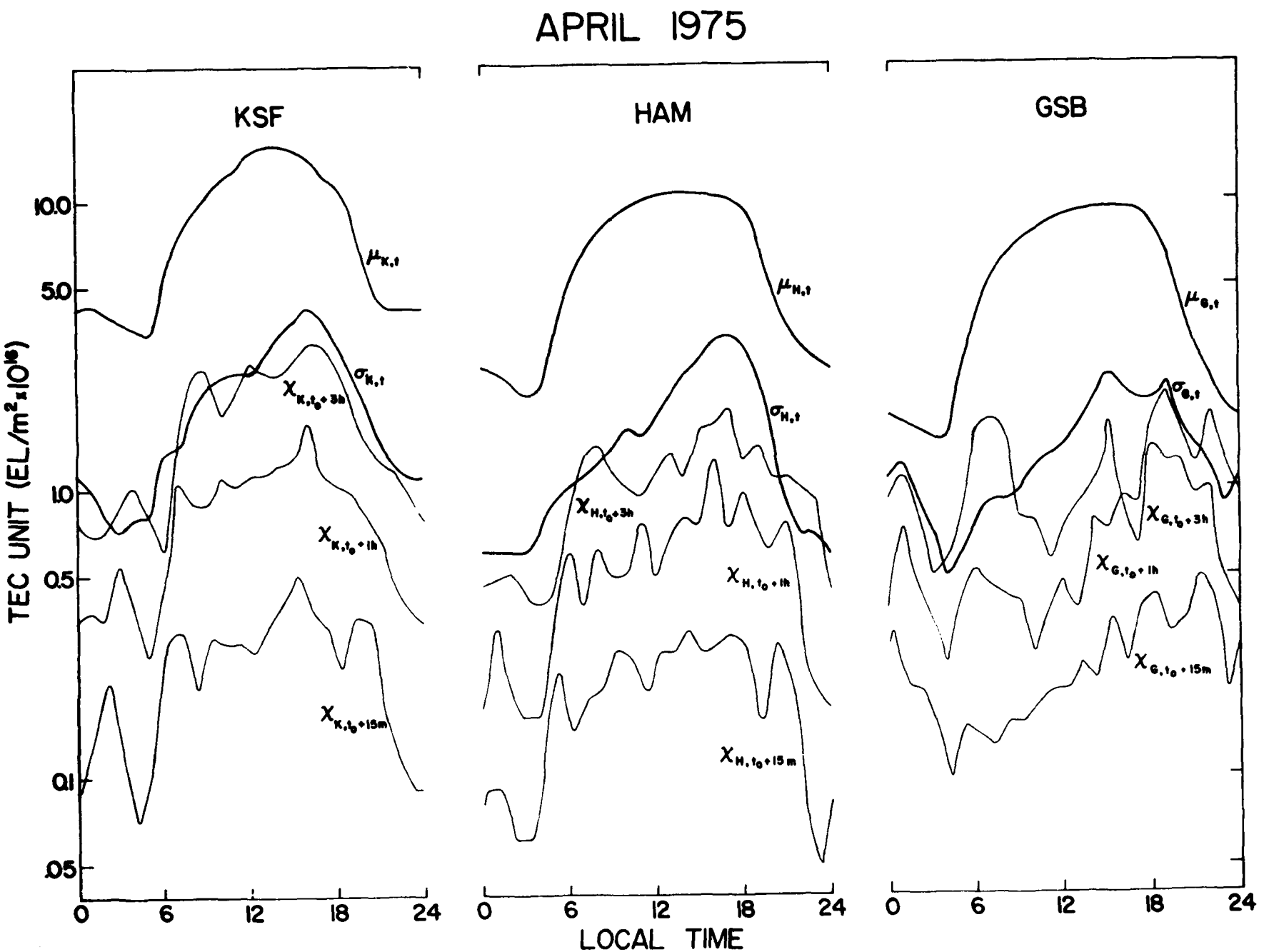
APRIL 1975
KSF
HAM
GSB
TEC UNIT (EL/m²x10¹⁶)
10.0
5.0
1.0
0.5
0.1
.05
$\mu_{K,t}$
$\sigma_{K,t}$
χ_{K,t_0+3h}
χ_{K,t_0+1h}
χ_{K,t_0+15m}
$\mu_{H,t}$
$\sigma_{H,t}$
χ_{H,t_0+3h}
χ_{H,t_0+1h}
χ_{H,t_0+15m}
$\mu_{G,t}$
$\sigma_{G,t}$
χ_{G,t_0+3h}
χ_{G,t_0+1h}
χ_{G,t_0+15m}
0
6
12
18
24
LOCAL TIME

FIGURE 10a

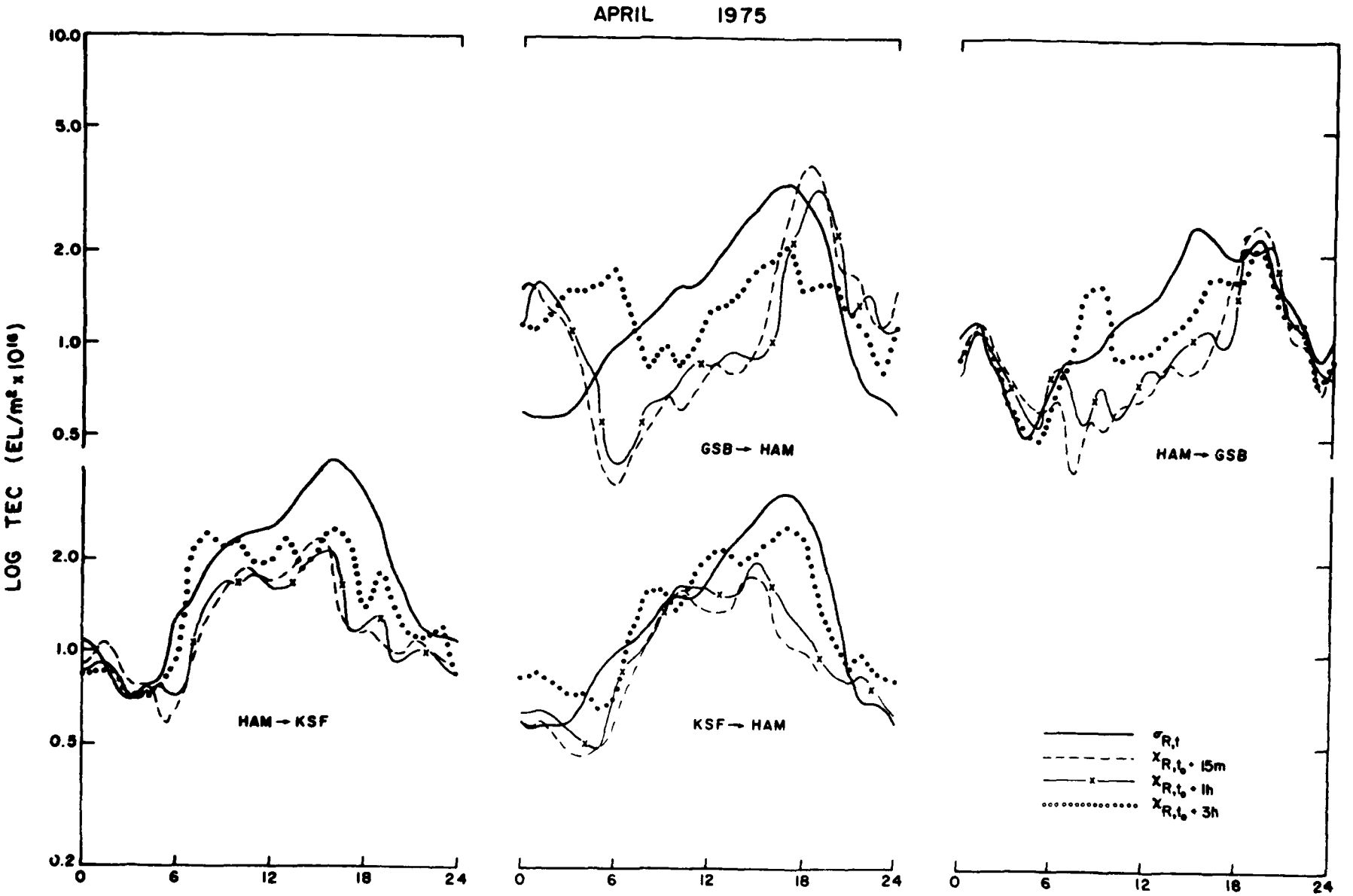
APRIL 1975
LOG TEC (EL/m² x 10¹⁶)
10.0
5.0
2.0
1.0
0.5
2.0
1.0
0.5
0.2
HAM → KSF
GSB → HAM
KSF → HAM
HAM → GSB
0
6
12
18
24
LOCAL TIME
σR,t
XR,t0 = 15m
XR,t0 = 1h
XR,t0 = 3h

FIGURE 10b

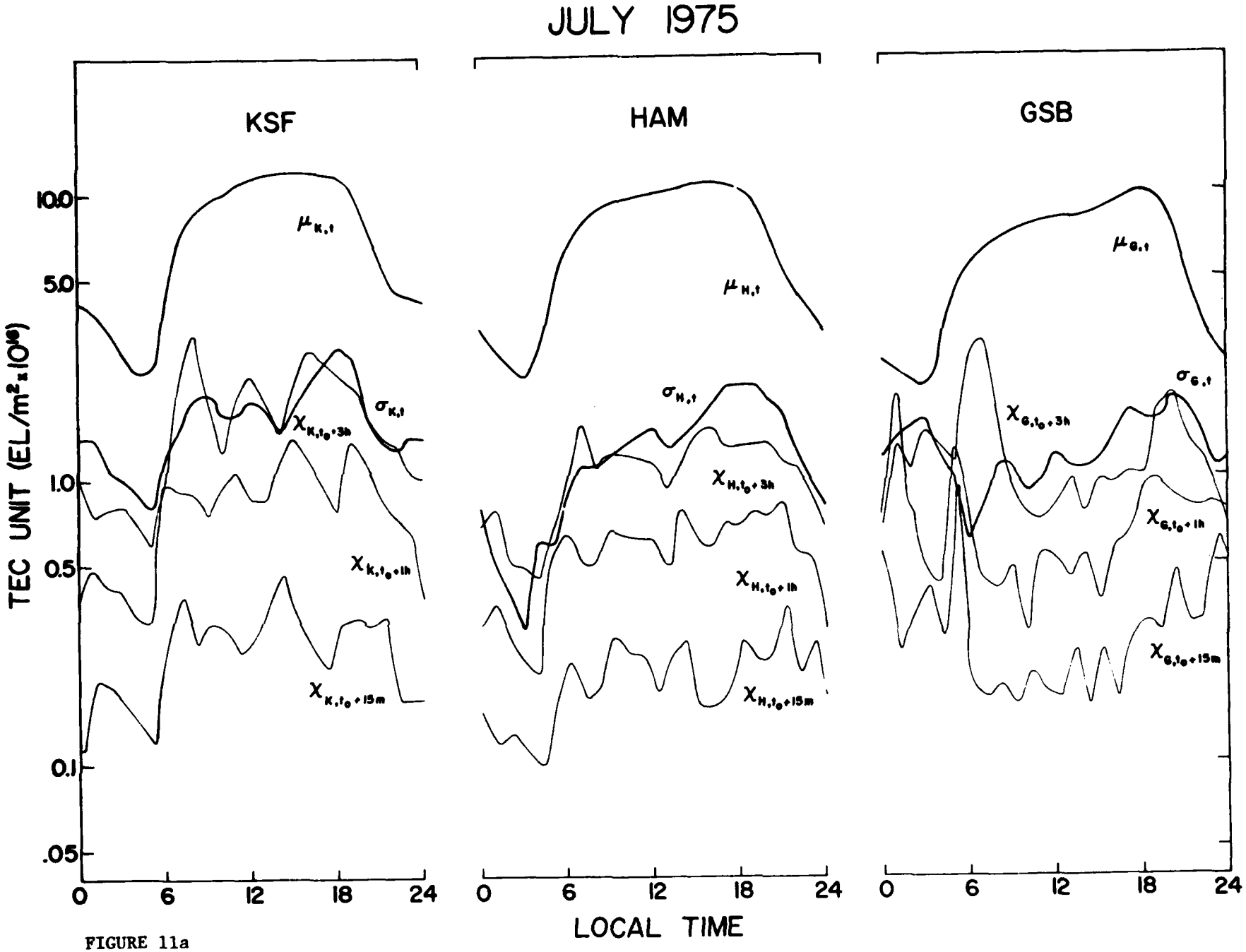
JULY 1975
KSF
HAM
GSB
TEC UNIT (EL/m² x 10¹⁶)
10.0
5.0
1.0
0.5
0.1
.05
$\mu_{K,t}$
$\sigma_{K,t}$
χ_{K,t_0+3h}
χ_{k,t_0+1h}
χ_{K,t_0+15m}
$\mu_{H,t}$
$\sigma_{H,t}$
χ_{H,t_0+3h}
χ_{H,t_0+1h}
χ_{H,t_0+15m}
$\mu_{G,t}$
$\sigma_{G,t}$
χ_{G,t_0+3h}
χ_{G,t_0+1h}
χ_{G,t_0+15m}
0
6
12
18
24
LOCAL TIME

FIGURE 11a

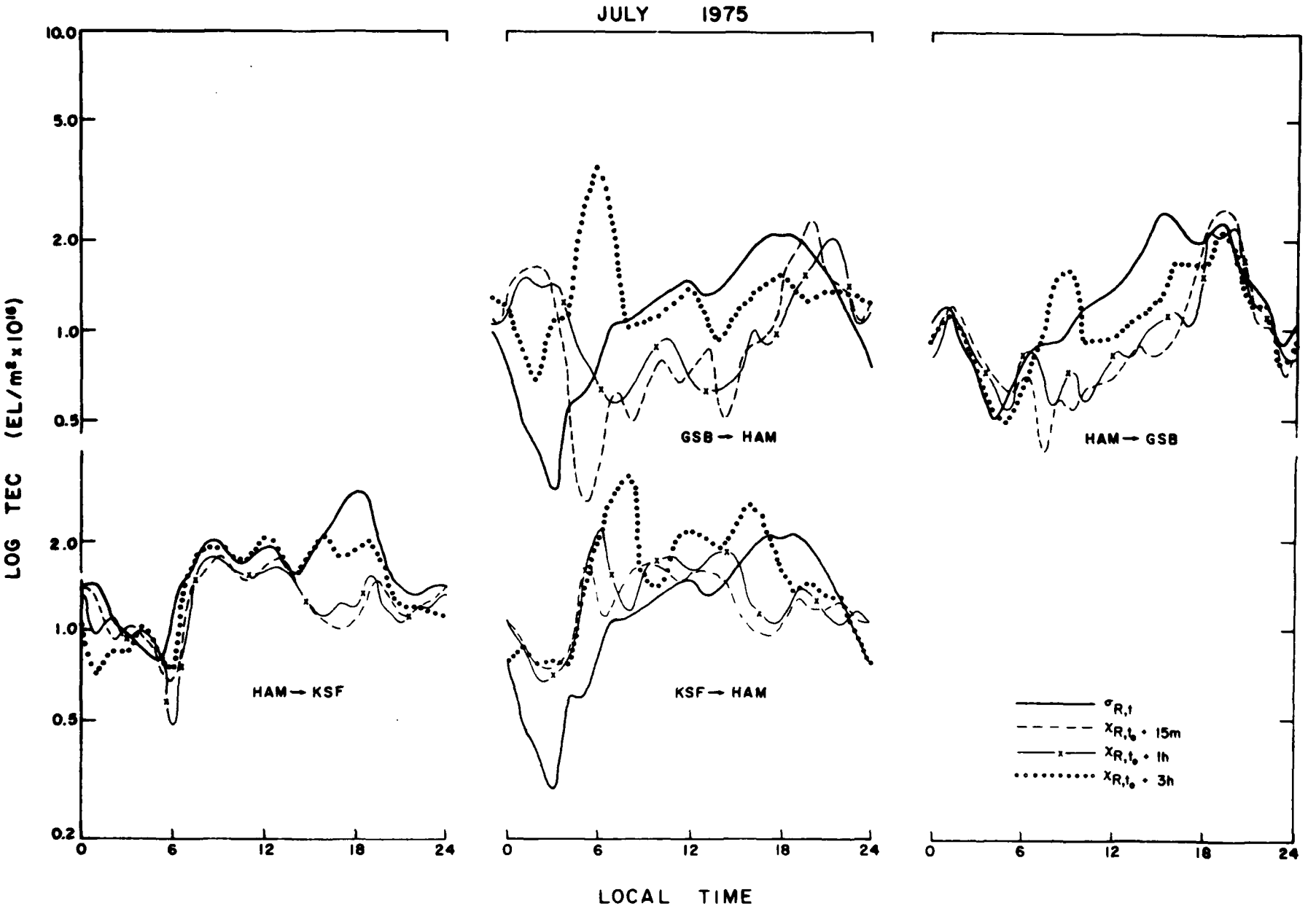
JULY 1975
LOG TEC (EL/m² x 10¹⁶)
10.0
5.0
2.0
1.0
0.5
2.0
1.0
0.5
0.2
HAM → KSF
GSB → HAM
KSF → HAM
HAM → GSB
$\sigma_{R,t}$
x_{R,t_0} + 15m
x_{R,t_0} + 1h
x_{R,t_0} + 3h
0
6
12
18
24
LOCAL TIME

FIGURE 11b

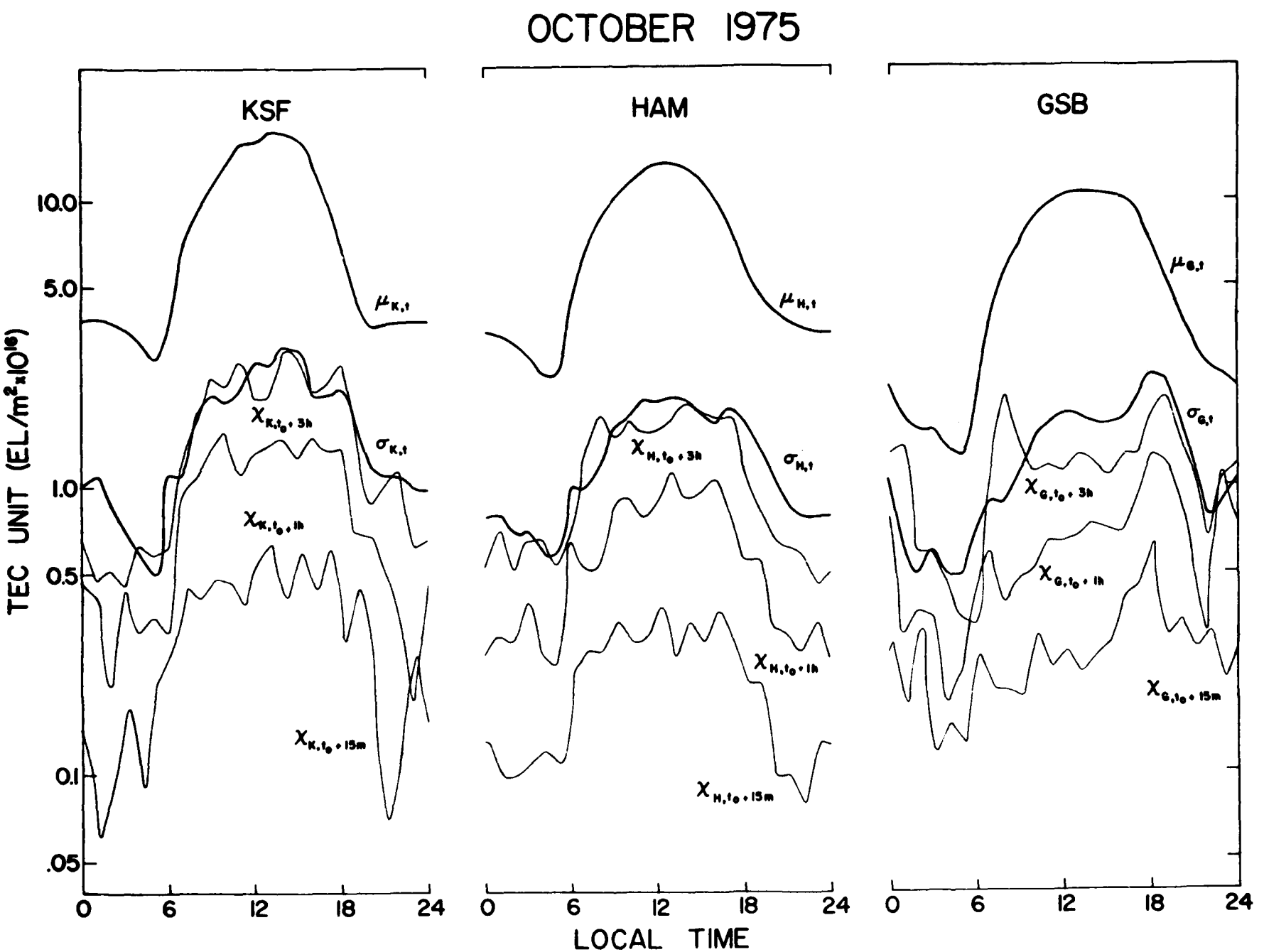
OCTOBER 1975
KSF
HAM
GSB
TEC UNIT (EL/m²x10¹⁶)
10.0
5.0
1.0
0.5
0.1
.05
$\mu_{K,t}$
$\mu_{H,t}$
$\mu_{G,t}$
$\sigma_{K,t}$
$\sigma_{H,t}$
$\sigma_{G,t}$
χ_{K,t_0+3h}
χ_{K,t_0+1h}
χ_{K,t_0+15m}
χ_{H,t_0+3h}
χ_{H,t_0+1h}
χ_{H,t_0+15m}
χ_{G,t_0+3h}
χ_{G,t_0+1h}
χ_{G,t_0+15m}
0
6
12
18
24
LOCAL TIME

FIGURE 12a

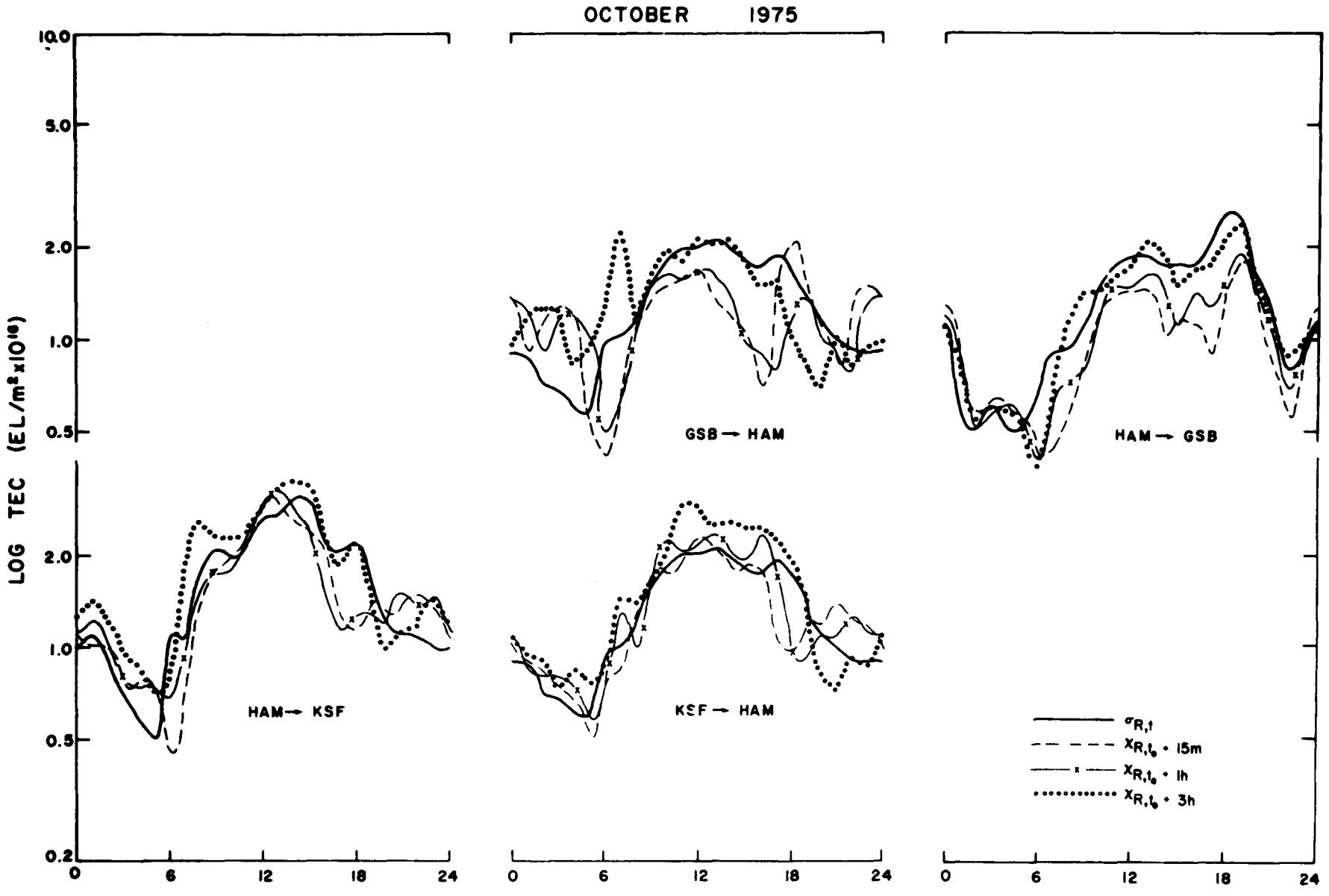
OCTOBER 1975
LOG TEC (EL/m²x10¹⁶)
10.0
5.0
2.0
1.0
0.5
2.0
1.0
0.5
0.2
HAM→ KSF
GSB→ HAM
KSF→ HAM
HAM→ GSB
σR,t
XR,t₀ + 15m
XR,t₀ + 1h
XR,t₀ + 3h
0
6
12
18
24
LOCAL TIME

FIGURE 12b